AN ADVANCE DISTRIBUTED CONTROL DESIGN FOR WIDE-AREA POWER SYSTEM STABILITY

by

Ibrahem E. Atawi

B.S., King Fahad University of Petroleum and Minerals, 2005

M.S., Florida Institute of Technology, 2008

Submitted to the Graduate Faculty of

the Swanson School of Engineering in partial fulfillment

of the requirements for the degree of

Doctor of Philosophy

University of Pittsburgh

2013

UNIVERSITY OF PITTSBURGH

SWANSON SCHOOL OF ENGINEERING

This dissertation was presented

by

Ibrahem E. Atawi

It was defended on

April 8, 2013

and approved by

Zhi-Hong Mao, Ph.D., Associate Professor, Electrical and Computer Engineering Department

Gregory Reed, Ph.D., Associate Professor, Department of Electrical and Computer Engineering

Ching-Chung Li, Ph.D., Professor, Department of Electrical and Computer Engineering

William Stanchina, Ph.D., Professor, Department of Electrical and Computer Engineering

Mingui Sun, Ph.D., Professor, Department of Bioengineering

Dissertation Director: Zhi-Hong Mao, Ph.D., Associate Professor, Electrical and Computer Engineering Department

AN ADVANCE DISTRIBUTED CONTROL DESIGN FOR WIDE-AREA POWER SYSTEM STABILITY

Ibrahem E. Atawi, PhD

University of Pittsburgh, 2013

The development of control of a power system that supply electricity is a major concern in the world. Some trends have led to power systems becoming overstated including the rapid growth in the demand for electrical power, the increasing penetration of the system from renewable energy, and uncertainties in power schedules and transfers. To deal with these challenges, power control has to overcome several structural hurdles, a major one of which is dealing with the high dimensionality of the system.

Dimensionality reduction of the controller structure produces effective control signals with reduced computational load. In most of the existing studies, the topology of the control and communication structure is known prior to synthesis, and the design of distributed control is performed subject to this particular structure. However, in this thesis we present an advanced model of design for distributed control in which the control systems and their communication structure are designed simultaneously. In such cases, a structure optimization problem is solved involving the incorporation of communication constraints that will punish any communication complexity in the interconnection and thus will be topology dependent. This structure optimization problem can be formulated in the context of Linear Matrix Inequalities and ℓ_1-minimization.

Interconnected power systems typically show multiple dominant inter-area low-frequency oscillations which lead to widespread blackouts. In this thesis, the specific goal of stability control is to suppress these inter-area oscillations. Simulation results on large-scale power system are presented to show how an optimal structure of distributed control would be

designed. Then, this structure is compared with fixed control structures, a completely decentralized control structure and a centralized control structure.

Keywords: power system, control, distributed, inter-area oscillations.

TABLE OF CONTENTS

LIST OF TABLES

LIST OF FIGURES

PREFACE

My deep gratitude goes to Dr. Zhi-Hong Mao, who is my thesis supervisor. He has given me so much support not only in research but also in my life. His motivation, perspective, and hard work is appreciated, as it has enabled me to complete this thesis, and I am very proud to have him as my research adviser.

I would also like to thank my committee members, Dr. Gregory Reed, Dr. Ching-Chung Li, Dr. William Stanchina, and Dr. Mingui Sun, for all their suggestions and guidance. Also, my deepest gratitude goes to my beloved Mrs. Hanouf Atawi for her support and encouragement, and to my little two kids, Layan and Vayan. Moreover, my gratitude goes overseas back home, Saudi Arabia, to my mother, brothers, and sisters for their support.

1.0 INTRODUCTION

A power system is a small or large scale network that is used to supply and deliver electrical power to residential and commercial consumers. The development of control of a power system that supply electricity is a major concern in many countries such as the United States and countries in Europe. Over the last five decades power systems have continued to serve the growing needs of individuals and industry, but some trends in the filed of energy supply have led to the current power system network becoming overstressed [65].

The first of these trends is the rapid, ongoing increase in the demand for electrical power, as detailed in Figure 1a. In the U.S., from 2010 to 2035 the demand for electricity is expected to grow by 22 percent from 3,877 billion kilowatt-hours to 4,716 billion kilowatt-hours. Over the same period residential demand is expected to grow by 18 percent to 1,718 billion kilowatt-hours, and continued population shifts to climatically warmer regions that will require power systems to accommodate greater cooling requirements . In 2035, commercial demand is expected to increase by 28 percent to 1,699 billion kilowatt-hours. From 2010 to 2035 transportation demand is expected to increase from 7 billion kilowatt-hours to 22 billion kilowatt-hours. [3, 4]

The second trend that has led to the current power system network becoming overstressed is the increasing penetration of energy from renewable sources such as wind and solar energy. Wind energy constitutes the largest share of renewable energy, with expected increases from 99.7 billion kilowatts in 2005 to 1628.4 billion kilowatts in 2035 globally, as shown in 1b. Also, both solar energy and biomass energy, while starting off slower than wind energy, are expected to grow even more quickly. Overall, then, total renewable energy is expected to grow quite rapidly in the short term. [3, 4]

Finally, electrical power is transferred considerable distances through high voltage transmission systems, and these lines have flow limitations. Thus, there are large number of sources of uncertainty in the operation of a power system, in terms of schedules and transfers.

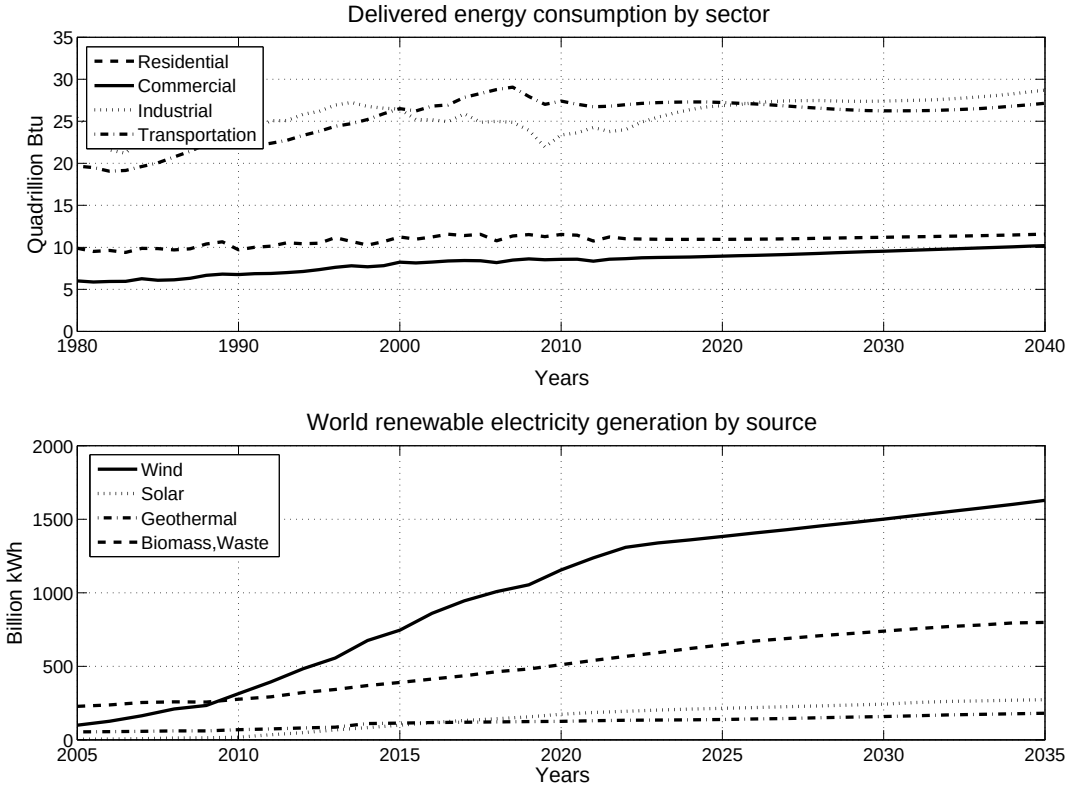

Figure 1: (a) U.S. energy consumption by sector (data from [4]). (b) World renewable electricity generation by source (data from [3])

To address these challenges, the power system network not only need to be upgraded with advanced hardware and equipment, but also must be reconfigured to make it smarter – capable of optimizing the use of the existing infrastructure while securing electrical service that is reliable, economical, efficient, safe, and environmentally responsible [46]. In order to

achieve the aforementioned benefits that the smart grid provides, power control has to overcome several structural hurdles, a major one of which is dealing with the high dimensionality of the control system.

2.0 LITERATURE REVIEW

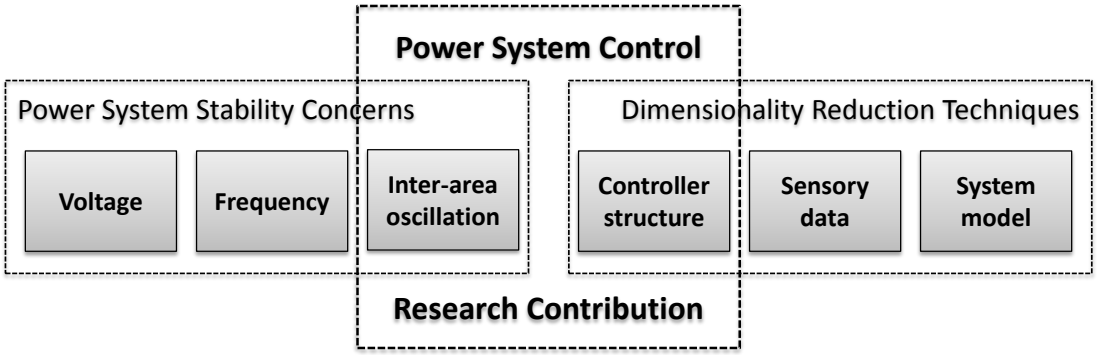

Figure 2: Research contribution

2.1 DIMENSIONALITY REDUCTION IN CONTROL OF A LARGE-SCALE SYSTEM

In the United States the power grid is a huge interconnected network, as shown in Figure 3. The North American network has between 10,000 and 100,000 nodes or branches and about 100 control centers [43]. The mathematical description of this network involves differential and algebraic equations with extraordinarily high dimensional variable space [76]. The network also requires the coordination of a large number of local actions on the part of the energy generation and transmission controllers [29]. Furthermore, this network exhibits a large range of characteristics, some which are highly nonlinear, such as bifurcation and chaos

[89]. These nonlinearities are generally hard to handle in control, even after simplification in modeling [61]. Moreover, a large-scale power system needs to be controlled under condition of distributed disturbances caused by noise and transmission delays scattered throughout the network.

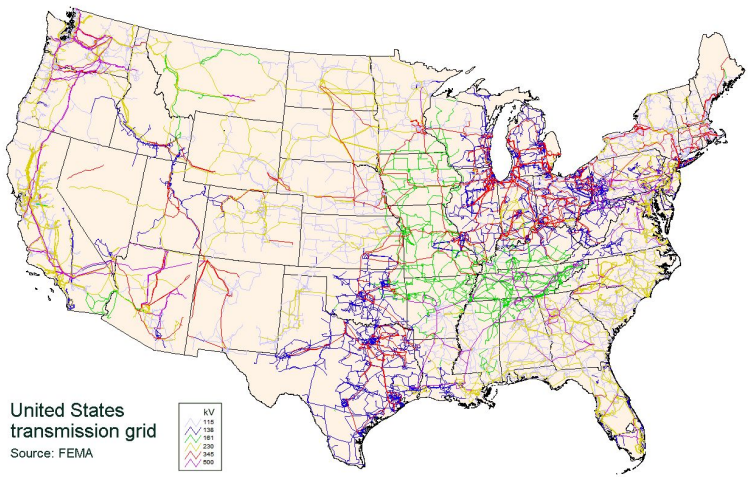

Figure 3: United Sates power network (figure adapted from [2]).

In control of a complex network, such as a large-scale power system, dimensionality reduction become essential to the computation of control signals in real time. The purpose of dimensionality reduction is to promote the efficiency and robustness of the power system by reducing the computational and communicational complexity of the control. Dimensionality reduction can be implemented for (i) the sensory data, (ii) the system model, and (iii) controller structure, respectively.

Dimensionality reduction of the sensory data aims to transform date of high dimensionality into a meaningful representation exhibiting reduced dimensionality, as shown in Figure 4. Techniques commonly used to achieve this goal include linear methods such as principle component analysis (PCA) [49] and multidimensional scaling (MSD) [28]. Examples of nonlinear methods are isomap [88], kernel (PCA) [83], diffusion maps [59], locally liner embedding [80], locally linear coordination [87], Laplacian eigenmaps[12], and manifold charting [19]. Sensory-data dimensionality reduction can also be achieved by directly reduc-

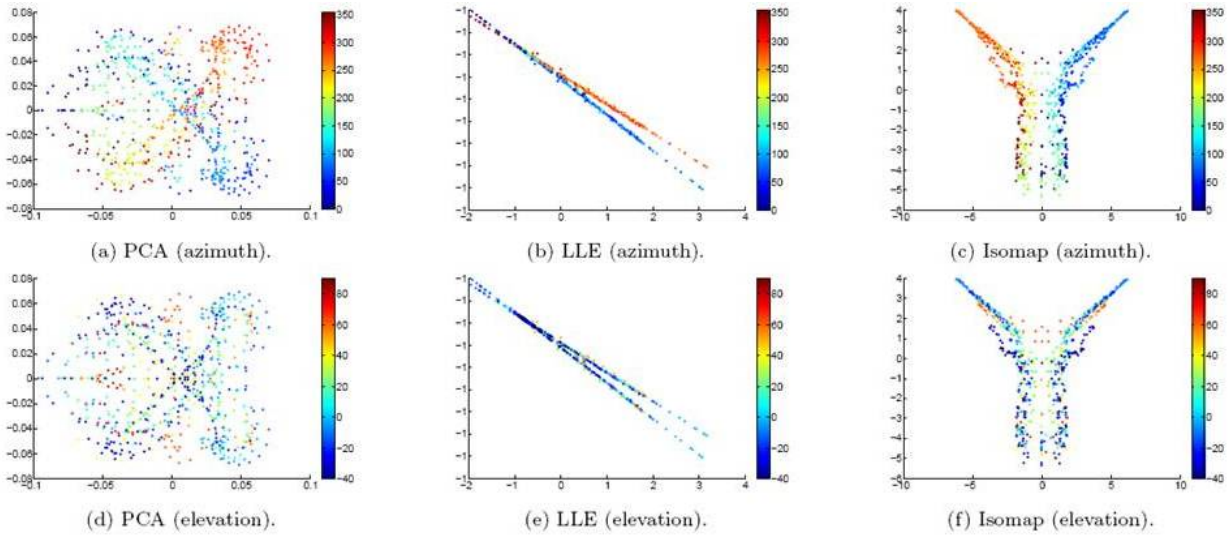

(a) PCA (azimuth). (b) LLE (azimuth). (c) Isomap (azimuth).

(d) PCA (elevation). (e) LLE (elevation). (f) Isomap (elevation).

Figure 4: Examples of dimensionality deduction methods for the sensory data.

ing the number of sensory channels or sampling rates. For example, in power system design, many research efforts have been made to determine optimal minimum sensor placements in the network [13, 21, 40, 75]. To reduce the sampling rate, a novel sampling, paradigmcompressive sensing, has been proposed, given that it can recover certain signals from far fewer samples than traditional methods can [22, 23, 33]. For data collection in networked control systems, compressive sensing can be realized in a decentralized manner [41, 10].

Dimensionality reduction of the system model aims to replace the original model with one of a much smaller dimension. The reduced model should be a sufficiently accurate approximation of the original model. One category of model-reduction methods is based on identifying and preserving certain modes of interest [24], e.g. modal model reduction [5, 16, 63]. Another category of these methods focuses on the observability and controllability properties of the system and is based on singular value decomposition (SVD) [7], e.g., balanced truncation [66] and Hankel norm approximation [47]. In addition, moment matching methods based on Krylov subspaces have been used for model reduction [6, 11, 24].

This thesis will focus only on the dimensionality reduction of the controller structure. This reduction technique aims to produce effective control signals with reduced computational load. In comparison with entirely centralized control, completely decentralized control has been a more popular choice of control architecture because of its ability to effectively solve the problems of dimensionality, uncertainty, and information structure constraints in large-scale systems [45]. Completely decentralized control most likely requires the weak interconnection assumption used in a large-scale network. A large body of existing literature has contributed to the development of distributed control for large-scale systems [48, 84, 91, 93]. In particular, the optimal design of distributed control has been widely studied since at least the 1970s [42, 81, 82]. In recent years, a trend has been to converge control, communication, and computation in the design of a distributed structure for networked control systems [8]. However, in most of the existing research, the topology of the control and communication structure are known prior to synthesis, and the optimal design for distributed control is performed subject to this particular structure. To the best of our knowledge, only Langbort and Gupta [55] have designed the controller and the topology the controller structure at the same time.

$$
\begin{aligned}
&\min \int_0^\infty X^T Q X + U^T R U \\
&\text{subject to} \\
&\dot{x}_i(t) = A_i x_i(t) + B_i u_i(t) \ \forall t > 0, \ \forall i = 1, \ldots, N \\
&x_i(0) = x_i^0
\end{aligned}
\tag{2.1}
$$

These researchers formulated the controller design as a linear quadratic regulation (LQR) problem, in which communication was indirectly reflected in their problem formulation by a topology dependent matrix in the LQR cost function, as shown in Equation (2.1). However, the effect of these communication constraints in control cannot be objectively and quantitatively evaluated. In this thesis, we will study the synthesis problem in the control structure and explicitly model the communication channels, considering time delay and uncertainties, and directly defining, in the cost function, a term that punishes communication complexity

within the controller structure. We will transform the structural optimization problem into a problem which seeks sparse solutions that can be solved using ℓ_1-minimization [32].

2.2 DAMPING CONTROL FOR INTER-AREA OSCILLATIONS

Power systems have a large number of generators and controllers, as well as many types of loads. The entry of more controllers and loads increase the complexity and nonlinearity of a power system. As a result, power systems are viewed as complex nonlinear systems that are vulnerable to a number of instability problems. In power systems, we can classify instability problems into three main types: voltage, phase, and frequency related problems [27, 31, 54, 56, 57, 58, 62, 71, 77, 79]. These instability problems may be studied separately for large-scale power systems. In this thesis, we will only focus on subclass of phase angle related instability problems.

The ability of synchronous machines in an interconnected power system to remain synchronize after being subjected to small disturbances is known as small signal stability, a type of phase angle instability problem. The performance of an interconnected power system depends on machine capability in order to maintain equilibrium between the electromagnetic torque and mechanical torque of synchronous machines. The unbalanced between electromagnetic torque and mechanical torque can be maintained into two mechanisms:

- A synchronizing torque component in phase with rotor angle deviation. The lack of sufficient synchronizing torque results in non-oscillatory instability.
- A damping torque component in phase with speed deviation. The lack of damping torque results in low frequency oscillations.

The main reason for oscillations in the power system is the unbalance between power demand and available power, which in turn causes an unbalance between electromagnetic torque and mechanical torque. Increasing and decreasing phase angle with a low frequency will be reflected in the goal of maximum power transfer and optimal power system security. Low frequency oscillations are generator rotor angle oscillations that have a frequency between 0.1 -2.0 Hz and are classified based on the source of the oscillation [54, 72] as follows:

- Local oscillation: This occurs because of the swinging of generators at power station against the rest of the power system, and happens to a small part of the power system. Normally, the range of the frequency is 1-2 Hz.
- Inter-area oscillation: This occurs because of the swinging of many generators in one part of power system against other generators in different parts of power system. Normally, the range of the frequency is 0.1-1 Hz.

In addition to these types of oscillation, there can be other types associated with the controllers, and are the result of poor design controllers [72]. Since the 1960s and 1970s, the conventional controllers for oscillation damping control include the automatic voltage regulator (AVR) [14], the power system stabilizer (PSS) [15], the speed governor [74], and the field excitation control [52]. These controllers are single-input single-output (SISO) controllers and work in a completely decentralized control structure. In a large-scale power system, the inter-area frequencies may fall well below 0.2 Hz while local oscillations may exceed 4 Hz [50]. Conventional SISO controllers cannot handle such a wide frequency range; consequently, many incidents related to low frequency oscillations have been reported [70]. For example, as a result of an incidence of LFO on August 14, 2003, a massive power outage occurred throughout eight northeastern and midwestern U.S. states, as well as Ontario, Canada, as shown in Figure 5.

In recent years, wide-area measurement systems (WAMS) using synchronized phase measurement units as shown in Figure 6 have been introduced into the design for damping control [25, 30, 34, 35, 51, 64, 68, 69, 95, 96]. Wide-area measurement systems with PMU have made it possible to implement centralized [92] and hierarchical control [34, 44, 51, 69] for oscillation damping. However, in all of the studies mentioned above, the structure of damping

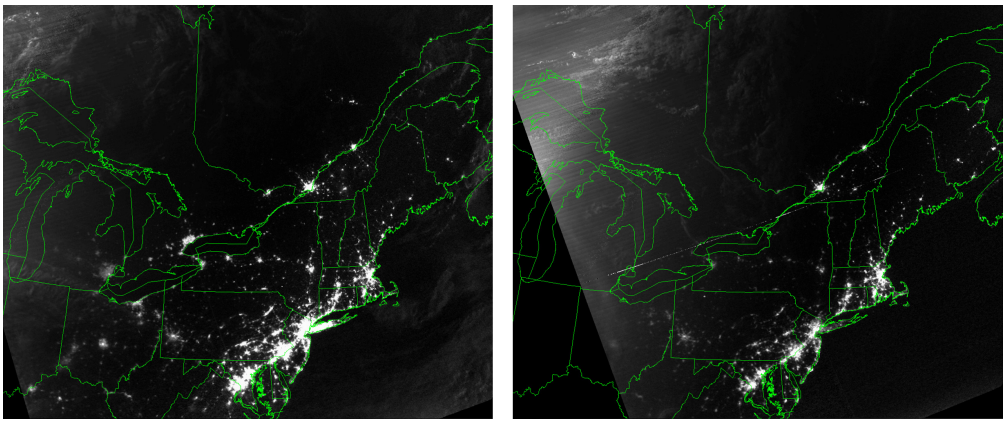

Figure 5: Northeast and midwestern U.S. states blackout of 2003. (Left satellite image) shows light activity on August 14 at 9:29 p.m. EDT about 20 hours before blackout. (Right satellite image) shows light activity on August 15 at 9:14 p.m. EDT about 7 hours after blackout (figure adapted from [1]).

control is fixed, and the controller design is subjected to a fixed structure. In this thesis, we present and demonstrate a hierarchical control system and control-communication co-design for hundling inter-area oscillations in the damping control. Our controller structure has the advantages of being synthesizeable and optimizable, taking into consideration of the cost due to communication delays and data losses.

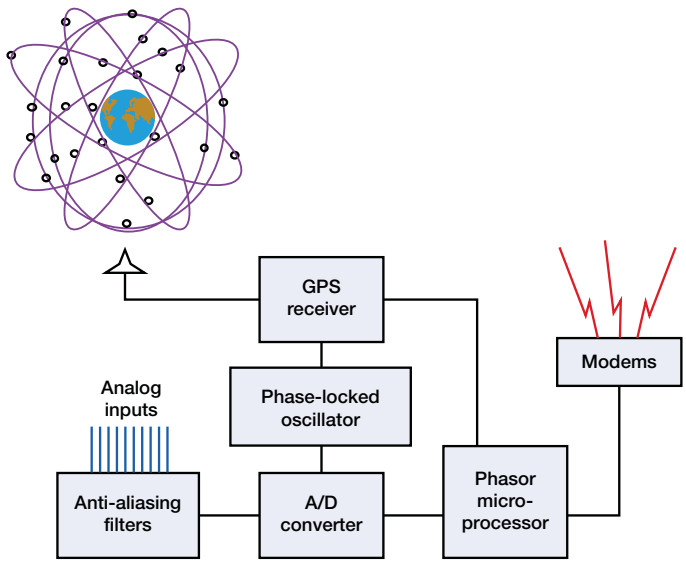

Figure 6: Block diagram of the Phasor Measurement Unit (figure adapted from [30]).

3.0 OBJECTIVE

3.1 INTRODUCTION

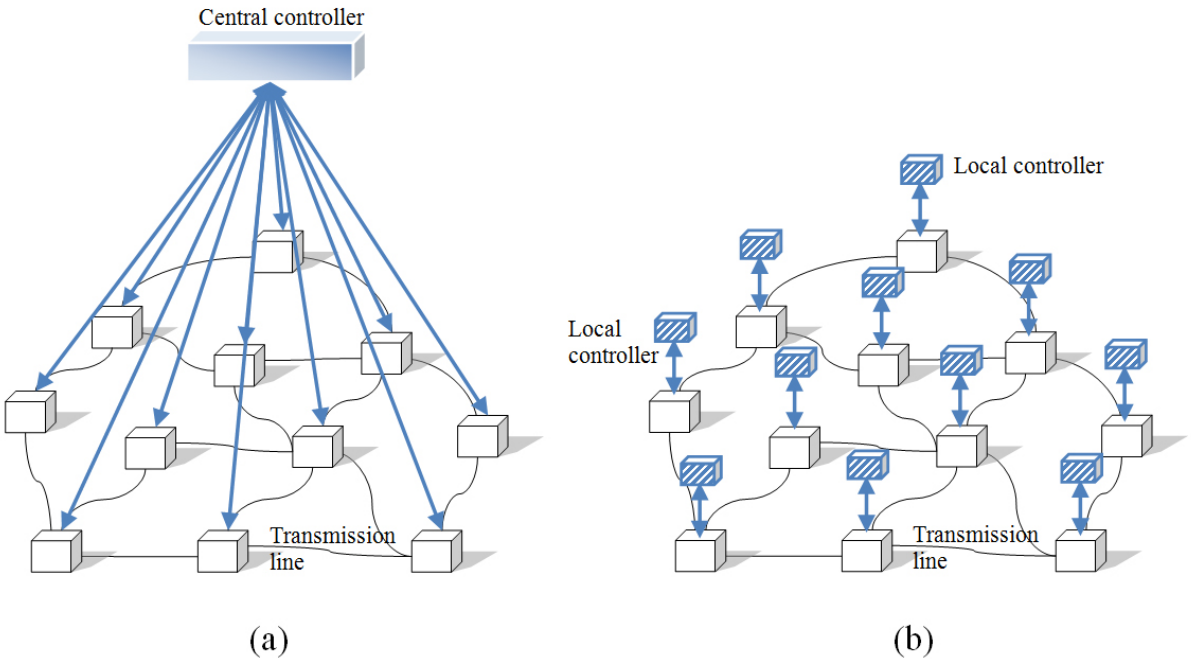

Figure 7: (a) Centralized control structure in a large-scale power system. (b) Completely decentralized control structure in a large-scale power system.

The control structure for a complex network such as a large scale power system can be classified as one of three main structures: a centralized structure, a completely decentralized structure, or a distributed structure. Centralized control, as shown in Figure 7a, would entail having a single controller measure all outputs of the power system, compute all the optimal

control input, and apply this control to all areas in one optimization problem. For a large-scale system such as a power system, it would be decidedly unreasonable to implement a centralized controller. A completely decentralized control system employs a single controller for each area with no communication between individual controllers as shown in Figure 7b. In this type of system, controllers ignore the interaction between the different subsystems. This type of structure may contribute to insufficient performance in power system control, especially if those subsystems are required to cooperate significantly in an interconnected power system. The third structure, distributed control, also involves a single controller for each subsystem, but, unlike the completely decentralized system, allows these subsystems to communicate with each other by sharing information.

Significantly in terms of, a large scale network such as a power system requires reducing the dimensionality inherent in the centralized configuration while avoiding the poor performance that can result from utilizing a completely decentralized configuration. This fact, along with the previously mentioned continuing increase in demand for electricity and the growing incorporation of renewable energy into the power system, has led many researchers to focus on distributed control in their search for a faster performing, more efficient control structure for large-scale power systems.

3.2 DESIGN OF A HIERARCHICAL ARCHITECTURE OF CONTROL WITH OPTIMAL TOPOLOGY

The main innovation of this section consists of reducing the dimensionality of control via minimizing the topology of the control and communication network needed to achieve a particular control goal. In most existing studies of hierarchical control, the interconnection topology is fixed. In our thesis, the distributed controllers and their connection topology are designed at the same time. Our structure optimization problem integrates control and communication in the design. Our hierarchical control architecture has two layers, as shown in Figure 8. The first layer is the decentralized layer, consisting of a distributed local controller similar to that which is presented in Figure 7b. However within the layer the

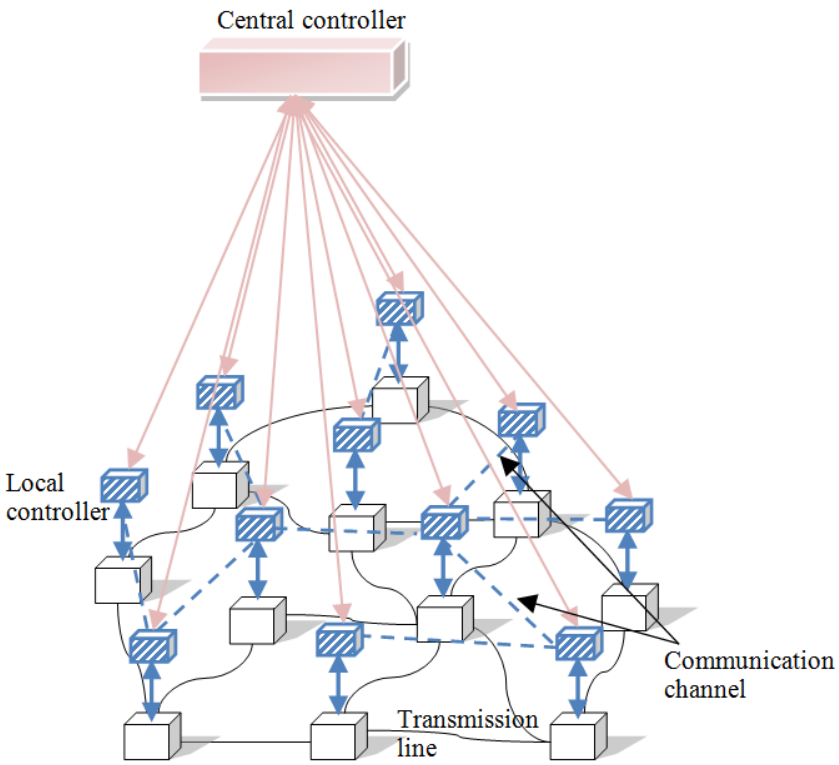

Figure 8: Illustration of our design of distributed control structure in a large-scale power system.

local controllers are allowed to connect and cooperate with one another. The connection structure of these controllers is a part of the design and needs to be determined by solving a structure optimization problem that involves incorporating a communication constraint, which will punish any communication complexity in the interconnection and thus will be topology dependent. This structure optimization problem can be formulated in the context of Linear Matrix Inequalities [18] and ℓ_1-minimization [32].

The second layer of our design is a single central controller, similar to the one presented in Figure 7a. However, the central controller in our method does not control the actuators directly. Rather, it supervises and coordinates the operation of the local controllers in the

first layer, adaptively optimizing the control and communication structure in real time. As a result, this central controller has greatly reduced responsibilities for control of the entire system.

3.3 DEMONSTRATION OF THE HIERARCHICAL CONTROL SYSTEM

In terms of the stabilization problem of the power system, the specific goal of stabilization is to suppress inter-area low frequency oscillations. Conventional controllers for power system stabilization include an automatic voltage regulator (AVR) [14], a power system stabilizer (PSS) [15], a speed governor [74], and a field excitation control [52]. These controllers are single-input single-output (SISO) linear controllers and work in a completely decentralized, non-cooperative manner; as a result, they cannot always guarantee stability when severe disturbances occur in the power system. Our solution utilization is a hierarchical control system that implements wide-area monitoring and control. Communication constraints will be considered to determine optimal connections among the local controllers. We compare the performance of our design with those having conventional designs and centralized control under communication constraints.

4.0 BACKGROUND

4.1 INTER-AREA OSCILLATIONS

4.1.1 Power System Modeling

In designing, an optimal topology of distributed control to suppress inter-area low frequency oscillation, we performed the steps presented here to obtain a dynamic model of a large scale power system. The notation is borrowed from [53]. When there is an unbalance between the mechanical torque (T_m) and electromagnetic torque (T_e), the net torque causing acceleration (or deceleration) is

$$T_a = T_m - T_e \tag{4.1}$$

where

T_a: acceleration motion torque $N \cdot m$.

T_m: mechanical torque $N \cdot m$.

T_e: electromagnetic torque $N \cdot m$.

In the above equation, T_m and T_e are positive for a generator and negative for a motor. The combined inertia of the generator and prime mover is accelerated by the unbalance of the applied torques. Hence, the equation of motion is

$$J\frac{d\omega_m}{dt} = T_a = T_m - T_e \tag{4.2}$$

where

J: the combined moment of inertia of the generator and turbine, $kg \cdot m^2$.

ω_m: the angular velocity of the rotor, rad/s.

The above equation can be normalized in terms of per unit inertia, using the constant H, defined as the kinetic energy in watt-seconds at the rated speed divided by the VA base. Using ω_{om} to denote the rated angular velocity in mechanical radians per second, the moment of inertia J in terms of H is

$$J = \frac{2H}{\omega_{0m}^2} VA_{base}. \tag{4.3}$$

Substituting the above in Equation (4.2) gives

$$\frac{2H}{\omega_{0m}^2} VA_{base} \frac{d\omega_m}{dt} = T_m - T_e. \tag{4.4}$$

If $T_{base} = \frac{VA_{base}}{\omega_{0m}}$, rewriting the above equation yields the following:

$$2H \frac{d(\omega_m/\omega_{0m})}{dt} = \frac{T_m - T_e}{T_{base}} = \overline{T}_m - \overline{T}_e \tag{4.5}$$

where $\overline{T}_m$ and $\overline{T}_e$ are mechanical and electrical torque per unit (p.u.), respectively.
In the above equation

$$\frac{\omega_m}{\omega_{0m}} = \frac{\omega/p_f}{\omega_0/p_f} = \frac{\omega}{\omega_0} = \overline{\omega} \tag{4.6}$$

where ω is the angular velocity of the rotor in electrical rad/s, ω_o is its rated value, and p_f is the number of filed poles.

Now we can rewrite Equation (4.5) as follows:

$$2H \frac{d\overline{\omega}}{dt} = \overline{T}_m - \overline{T}_e. \tag{4.7}$$

If δ is the angular position of the rotor in electrical radians with respect to a synchronously rotating reference and δ_0 is its value at $t = 0$,

$$\delta = \omega t - \omega_0 t + \delta_0. \tag{4.8}$$

Taking the time derivative of the above equation, we have

$$\frac{d\delta}{dt} = \omega - \omega_0 = \Delta\omega. \tag{4.9}$$

Based on Equation (4.6), we can write the above equation as

$$\frac{1}{\omega_0}\frac{d\bar{\delta}}{dt} = \Delta\overline{\omega}. \tag{4.10}$$

Subsequently, the per unit equations of motion of a synchronous machine can be written as:

$$\frac{d\overline{\omega}}{dt} = \frac{1}{2H}(\overline{T}_m - \overline{T}_e) \tag{4.11}$$

$$\frac{d\bar{\delta}}{dt} = \omega_0\Delta\overline{\omega} \tag{4.12}$$

where the mechanical torque ($\overline{T}_m$), electrical torque ($\overline{T}_e$), angular velocity (speed rotor) ($\overline{\omega}$) and angular position (frequency)($\bar{\delta}$) are in per unit (p.u.).

The block diagram form representation of Equations (4.11 and 4.12) is shown in Figure 9:

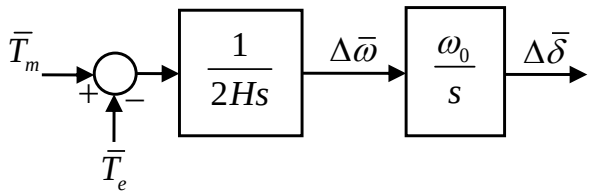

Figure 9: The frequency and torque relation.

In this thesis, we represent the frequency in terms of mechanical and electrical power. The relationship between the power and the torque is presented in [53, p.583]. Figure 10 expresses the frequency deviation output in terms of mechanical power and electrical power.

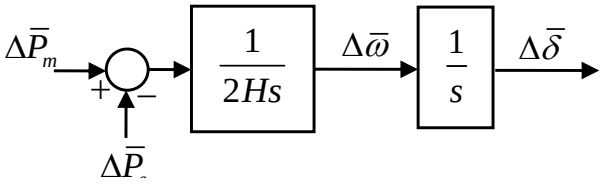

Figure 10: The frequency and power relation.

For some loads, such as motor loads, electrical power changes with the change in speed rotor. This type of load is dependent on speed rotor. However, the electrical power is independent of the speed rotor for resistive loads, such as lighting. Therefore, the electrical power can be express as follows:

$$\Delta\overline{P}_e = \Delta\overline{P}_L + D\overline{\omega} \tag{4.13}$$

where

$\Delta\overline{P}_L$: independent frequency load

$D\overline{\omega}$: frequency load

D: load damping constant.

The effect of load damping is showing in Figure 11.

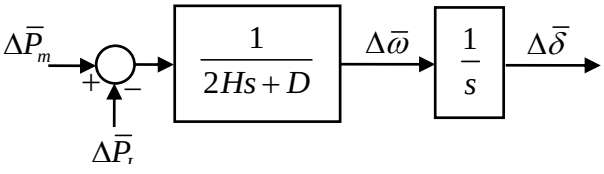

Figure 11: The frequency and load power relation.

A turbine is used to convert natural energy, such as water or steam, into mechanical power. In general, there are three common types of turbines used in power systems: reheat, non-reheat, and hydraulic. In all three types, the governor is the control unit of the power system. When the load on the system changes, the governor senses the frequency bias and cancels the change by adjusting the input of the turbines, which in turn changes the rotor speed. The turbine and governor can be represented in the transfer function as follows:

1. Turbine: (4.14)

(a) Non-reheat turbine: $T(s) = \dfrac{1}{T_{ch}s + 1}$

T_{ch} : time delay.

(b) Reheat turbine: $T(s) = \dfrac{F_{hp}T_{rh}s + 1}{(T_{ch}s + 1)(T_{rh}s + 1)}$

T_{rh} : low pressure reheat time. F_{hp} : high pressure stage rating.

(c) Hydraulic turbine: $T(s) = \left(\dfrac{T_R s + 1}{T_R(R_T/R)s + 1}\right)\left(\dfrac{-T_W s + 1}{(T_W/2)s + 1}\right)$

T_W : water starting time. T_R : reset time.

R_T : temporary droop. T : permanent droop.

2. Governor: $T(s) = \dfrac{1}{T_g s + 1}$ (4.15)

T_g : time constant of the governor.

For simplicity, a non-reheat turbine is chosen here to generate mechanical power. As such, the block diagram form including a turbine and governor is shown in Figure 12.

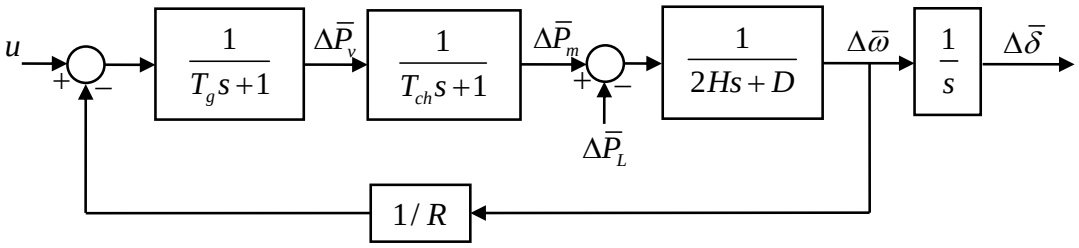

Figure 12: Block diagram of a power system.

where u is the input control signal.

Interconnected power system

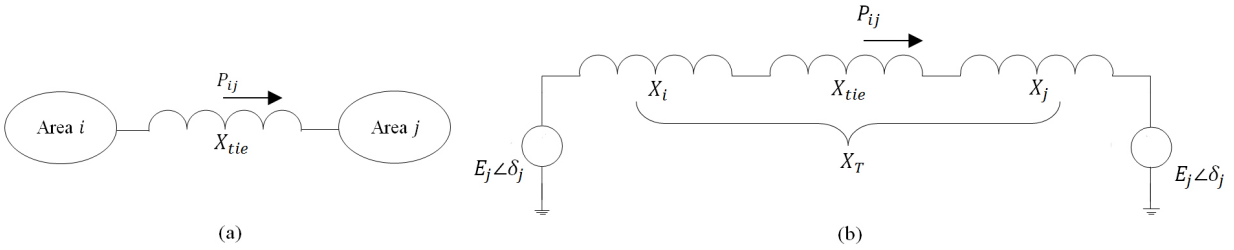

Figure 13: (a) Two-area system. (b) Electrical equivalent.

To form the basis for supplementary control of interconnected power systems, let us consider area i to be connected with area j by a tie-line of reactance X_{tie} as shown in Figure 13a. Figure 13b shows the electrical equivalent of the system. The power flow on the tie-line from area i to area j is

$$\overline{P}_{ij} = \frac{\overline{E}_i \overline{E}_j}{X_T} \sin(\overline{\delta}_i - \overline{\delta}_j) \tag{4.16}$$

where X_T is the equivalent of reactance.

Linearizing about an initial operation point, we have

$$\Delta\overline{P}_{ij} = T_{ij}\Delta\overline{\delta}_{ij} \tag{4.17}$$

where $\Delta\overline{\delta}_{ij} = \Delta\overline{\delta}_i - \Delta\overline{\delta}_j$, and T_{ij} is the synchronizing torque coefficient given as

$$T_{ij} = \frac{\overline{E}_i\overline{E}_j}{X_T}\cos(\overline{\delta}_i - \overline{\delta}_j). \tag{4.18}$$

The block diagram for i power system connected to j power system by the tie-line power can be modeled as shown in Figure 14.

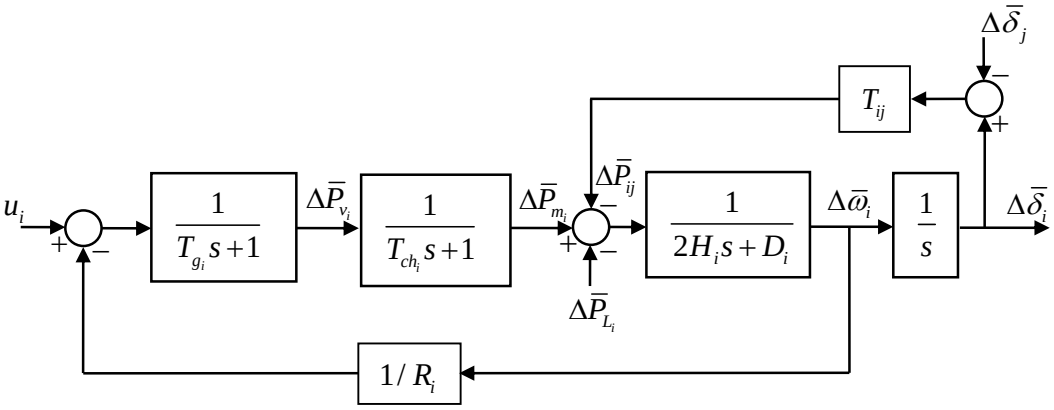

Figure 14: Block diagram of one area of an interconnected power system.

To simplify notation, we replace the stated variable symbols $\overline{\omega}$, $\overline{P}_{ij}$, $\overline{P}_m$ and $\overline{P}_v$ with ω, P_{ij}, P_m and P_v throughout the thesis, but all stated variables still per unit. Considering area i to be connected to more than one area j; the dynamic model of area i in state-space form can be is given as follows:

$$\begin{bmatrix} \Delta\dot{\omega}_i(t) \\ \Delta\dot{P}_{ij}(t) \\ \Delta\dot{P}_{m_i}(t) \\ \Delta\dot{P}_{v_i}(t) \end{bmatrix} = \begin{bmatrix} -\frac{D_i}{2H_i} & -\frac{1}{2H_i} & \frac{1}{2H_i} & 0 \\ \sum_{i\neq j} T_{ij} & 0 & 0 & 0 \\ 0 & -\frac{1}{T_{ch_i}} & 0 & \frac{1}{T_{ch_i}} \\ -\frac{1}{T_{g_i}R_i} & 0 & 0 & -\frac{1}{T_{g_i}} \end{bmatrix} \begin{bmatrix} \Delta\omega_i(t) \\ \Delta P_{ij}(t) \\ \Delta P_{m_i}(t) \\ \Delta P_{v_i}(t) \end{bmatrix} + \begin{bmatrix} 0 \\ 0 \\ 0 \\ \frac{1}{T_{g_i}} \end{bmatrix} u_i(t) + \sum_{i\neq j} \begin{bmatrix} 0 & 0 & 0 & 0 \\ -T_{ij} & 0 & 0 & 0 \\ 0 & 0 & 0 & 0 \\ 0 & 0 & 0 & 0 \end{bmatrix} \begin{bmatrix} \Delta\omega_j(t) \\ \Delta P_{ji}(t) \\ \Delta P_{m_j}(t) \\ \Delta P_{v_j}(t) \end{bmatrix} \tag{4.19}$$

or

$$\dot{x}_i(t) = A_{ii}x_i(t) + B_i u_i(t) + \sum_{i\neq j} A_{ij}x_j(t) \tag{4.20}$$

where $x_i = [\Delta\omega_i, \Delta P_{ij}, \Delta P_{m_i}, \Delta P_{v_i}]^T$ is the local state variables, u_i is local control input, and $x_j = \left[\Delta\omega_j, \Delta P_{ji}, \Delta P_{m_j}, \Delta P_{v_j}\right]^T$ is the neighbor state variables.

Generally, we can write the dynamic model of a power system under a centralized structure as follows:

$$\begin{bmatrix} \dot{x}_1(t) \\ \dot{x}_2(t) \\ \vdots \\ \dot{x}_N(t) \end{bmatrix} = \begin{bmatrix} A_{11} & A_{12} & \dots & A_{1N} \\ A_{21} & A_{22} & \dots & A_{2N} \\ \vdots & \vdots & \ddots & \vdots \\ A_{N1} & A_{N2} & \dots & A_{NN} \end{bmatrix} \begin{bmatrix} x_1(t) \\ x_2(t) \\ \vdots \\ x_N(t) \end{bmatrix} + \begin{bmatrix} B_1 & 0 & \dots & 0 \\ 0 & B_2 & \dots & 0 \\ \vdots & \vdots & \ddots & \vdots \\ 0 & 0 & \dots & B_N \end{bmatrix} \begin{bmatrix} u_1(t) \\ u_2(t) \\ \vdots \\ u_N(t) \end{bmatrix} \tag{4.21}$$

where x is the state vector, u is the control input vector, and N is the total number subsystems. A_{ii}, A_{ij}, and B_i ($i = 1, \cdots, N$, $j = 1, \cdots, N$, and $i \neq j$) can be constructed as in Equation (4.19).

4.1.2 Eigenvalues Stability Analysis

The special interest of this thesis is inter-area low-frequency oscillation. As previously mentioned, the unbalanced between power demands and available power can create low frequency oscillations in the power system. Low frequency oscillations are normally analyzed in a power system in steady state as creating small disturbances. By looking to the eigenvalues of the A matrix in Equation (4.21), we can analyze the steady state stability of the system. The eigenvalues of A are given as follows:

$$(A - \lambda I)\nu = 0 \tag{4.22}$$

where λ is the eigenvalues and ν is the eigenvectors. The number of eigenvalues depends on the dimensions of matrix A or the number of state variables considered in the system. All the eigenvalues should be located in the open left half plane, in order to suppress oscillations in the power system. The system will be unstable if any of the real part of the eigenvalues are positive. Moreover, the damping ratio should be positive and in excess of critical value. The eigenvalues are given in the complex form ($\lambda = -a \pm b$); the damping ratio is defined as follows:

$$\zeta = \frac{-a}{\sqrt{a^2 + b^2}} \tag{4.23}$$

How to accurately define the critical value for the damping ratio is not clearly known, but according to how utilities operate in practice, damping ratio should be at least 5 percent. Therefore, in order to suppress oscillations in the power system the real part of the eigenvalues should be negative and the damping ratio should be positive critical value grater than 5 percent.

4.2 OPTIMIZATION TECHNIQUES

4.2.1 Linear Matrix Inequality

Linear Matrix Inequality (LMI) is a form of convex optimization used to solve problems in system and control theory. LMI helps to convert very large control problems to standard

convex optimization problems, which can then be solved efficiently and capably. The history of LMI began when Lyapunov demonstrated that the differential equation

$$\frac{d}{dt}x = Ax(t) \tag{4.24}$$

is stable if and only if there exits P such that

$$P > 0 \quad \text{and } A^T P + PA < 0. \tag{4.25}$$

Equation (4.25) is a special form of an LMI which can be analytically solved. Thus, the oldest form of LMI problem was to analyze the stability of a system by using Lyapunov theory. Subsequently, LMI has been developed and implemented in solving control problems with extreme efficiency. More recently, Nesterov and Nemirovskii [67] developed a interior-point method that applied Linear Matrix inequalities to convex problems.

A linear matrix inequality (LMI) has the form

$$F(x) \equiv F_0 + \sum_{i=1}^{m} x_i F_i \tag{4.26}$$

where $x \in R^m$ is the variable and the symmetric matrices $F_i = F_i^T \in R^{nxn}$,$i = 0, ..., m$, are given. The LMI in Equation (4.26) is a convex constraint on x, i.e., the set $\{x|F(x) > 0\}$ is convex. In their book, *Linear Matrix Inequalities (LMI) in System and Control Theory* [17], Boyd et al. have shown some problems of system and control theory, demonstrating how to decrease the size of convex optimization problems that involve inequality matrices.

In this thesis, we apply efficient tools such as Linear Matrix Inequalities (LMI) to power system control problems which have a great variety of control design requirements, such as the size and structure of the feedback gain matrix, communication and time delay constraints, and the degree of exponential stability. LMI has provided a great flexibility in dealing with these types of control problems. Furthermore, a guide on how to implement LMI in MATLAB can be found in *LMI Control Toolbox* [36].

4.2.2 ℓ_1-Minimization

Most control engineers prefer to represent data in the most parsimonious terms possible. In stability control problems specifically, they consider designing the feedback gain matrix as sparsely as feasible in certain controller structures, such as in distributed control. For example, solving stability problems under different controller structures is accomplished by finding the feedback gain matrix K such as in the following:

$$P > 0 \text{ and } (A + BK)^T P + P(A + BK) < 0. \tag{4.27}$$

Under different controller structures, the ℓ_0 norm $\|K\|_0$ is simply the number of nonzero in K. The optimal solution involves finding sparsest feedback gain by solving the optimization problem:

$$\min \|K\|_0 \text{ subject to } P > 0 \text{ and } (A + BK)^T P + P(A + BK) < 0 \tag{4.28}$$

The difficulty of solving above optimization problem is that it requires enumeration subsets of the library A. The computational complexity of such a subset search grows exponentially with increasing dimension of K. In order to deal with this difficulty, consider replacing ℓ_0-minimization in above optimal problem with ℓ_1-minimization, by replacing $\|K\|_0$ with $\|K\|_1$. After doing so, we can rewrite the stabilization optimization problem as

$$\min \|K\|_1 \text{ subject to } P > 0 \text{ and } (A + BK)^T P + P(A + BK) < 0 \tag{4.29}$$

where $\|K\|_1 = \sum_i \sum_j |K_{ij}|$, the sum of the absolute values of all elements of K.

The ℓ_1-minimization $\|K\|_1$ in the above optimization problem can be considered a kind of convexitaion of the problem of minimizing $\|K\|_0$. The added benefit of ℓ_1-minimization is that this can be cast of as linear programming problem and can be solved by modern interior point methods.

5.0 DESIGN METHODS

This thesis aims to find an optimal topology of distributed control, which is required in order to achieve a particular control goal. We propose to use two layers of hierarchical control architecture, shown in Figure 8. The first layer is a distributed control layer consisting of local controllers that can cooperate with each other. The advantage of these controllers and their interconnected topology is that they are designed at the same time by solving a structure optimization problem. This structural optimization problem aims to integrate the communication perspective in control system design. The cost function of the optimization problem includes a term that punishes the communication complexity of controller interconnection topology. The second layer of the hierarchical control architecture is a single central controller that coordinates the operations of the local controllers in the first layer and adaptively optimizes and updates the control and communication topology in real time.

This thesis involves the completion of three tasks. The first two tasks serve as preparation for the third, i.e., the main task, which aims to formulate and solve the structure optimization problem for controller structure synthesis.

5.1 TASK I: FORMULATING AND SOLVING THE SYSTEM STABILIZATION PROBLEM FOR VARIOUS CONTROL STRUCTURES

We start with this task in order to evaluate and develop intuitions about the performance and computational loads of various controller structures in stabilizing a power system. This task also provides us with opportunities to practice the system modeling and design, through

which we can gain insights that will be valuable when dealing with more complex and difficult design problems.

5.1.1 System Model.

As described in Section (4.1.1), under a centralized structure, the dynamic of a power system can be modeled as follows:

$$\dot{x}(t) = Ax(t) + Bu(t) \tag{5.1}$$

or

$$\begin{bmatrix} \dot{x}_1(t) \\ \dot{x}_2(t) \\ \vdots \\ \dot{x}_N(t) \end{bmatrix} = \begin{bmatrix} A_{11} & A_{12} & \dots & A_{1N} \\ A_{21} & A_{22} & \dots & A_{2N} \\ \vdots & \vdots & \ddots & \vdots \\ A_{N1} & A_{N2} & \dots & A_{NN} \end{bmatrix} \begin{bmatrix} x_1(t) \\ x_2(t) \\ \vdots \\ x_N(t) \end{bmatrix} + \begin{bmatrix} B_1 & 0 & \dots & 0 \\ 0 & B_2 & \dots & 0 \\ \vdots & \vdots & \ddots & \vdots \\ 0 & 0 & \dots & B_N \end{bmatrix} \begin{bmatrix} u_1(t) \\ u_2(t) \\ \vdots \\ u_N(t) \end{bmatrix} \tag{5.2}$$

where x is the state vector, u is the control input vector, and N is the total number of subsystems. A_{ii}, A_{ij}, and B_i ($i = 1, \cdots, N$, $j = 1, \cdots, N$, and $i \neq j$) can be constructed as in Equation (4.19).

5.1.2 Controller Structure.

Under the centralized architecture of the control, shown in Figure 7a, we consider the most commonly used control law-constant gain, full state feedback control [26]:

$$u(t) = Kx(t) \tag{5.3}$$

where $K = \begin{bmatrix} K_{11} & K_{12} & \dots & K_{1N} \\ K_{21} & K_{22} & \dots & K_{2N} \\ \vdots & \vdots & \ddots & \vdots \\ K_{N1} & K_{N2} & \dots & K_{NN} \end{bmatrix}$.

The system under control can now be described by the equation:

$$\dot{x}(t) = (A + BK)x(t) \tag{5.4}$$

In cases of completely decentralized or distributed control architecture as in Figure 7b or 8, the control law has the form

$$u(t) = K_D x(t) \tag{5.5}$$

where K_D is a sparse matrix with many zero elements. Note that different controller structures can be indicated by different nonzero patterns of the control gain matrices. Under centralized control, the state feedback gain matrix as, in Equation (5.3), is not sparse. This can be seen in Figure 15a. In contrast, with a completely decentralized structure as in Figure 15b, the gain matrix shown in Equation (5.5) is a block diagonal matrix. For a distributed structure, it forms an overlapping structure where each local controller shares information with its respective neighboring subsystem but not with the overall subsystem, as in the example shown in Figure 15c.

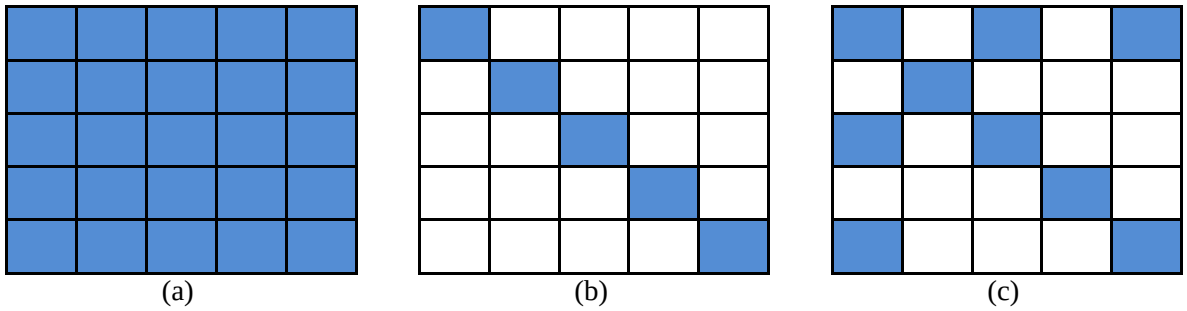

Figure 15: Gain matrix structures of a (a) centralized (b) completely decentralized (c) distributed control structure.

5.1.3 Stabilization

In this study, the specific control problem in which we are interested is the stabilization problem. Let us first consider the centralized control. To ensure the global asymptotic stability of the closed loop system (Equation (5.4)), we search for a control gain K and Lyapunov function

$$V(x) = x^T P x \tag{5.6}$$

with matrix P being symmetric so that

$$P > 0 \text{ and } (A + BK)^T P + P(A + BK) < 0. \tag{5.7}$$

Note that in Equation (5.7), P and K are not linear, so it is generally difficult to solve this matrix inequality. To avoid such difficulty, we follow a procedure proposed in [38, 93] and introduce new matrices:

$$Y = \tau P^{-1} \ (\tau > 0) \text{ and } L = KY \tag{5.8}$$

with which we can rewrite Equation (5.7) as

$$Y > 0 \text{ and } YA^T + AY + L^T B^T + BL < 0. \tag{5.9}$$

Any feasible Y and L which is subject to the above inequalities can produce a control gain matrix

$$K = LY^{-1} \tag{5.10}$$

which ensures global asymptotically in the stability of the system (5.4). In order to prevent $\|K\|_2$ from becoming unacceptably large, we need to add conditions to bound the norm of K . We therefore introduce the following inequality about L and Y to bound $\|K\|_2$ implicitly:

$$\begin{bmatrix} -\kappa_L I & L^T \\ L & -I \end{bmatrix} < 0 \text{ and } \begin{bmatrix} Y & I \\ I & \kappa_Y I \end{bmatrix} > 0 \tag{5.11}$$

where κ_L and κ_Y represent scalar variables.

Use of the Schur complement formula [18] reveals that matrix (5.11) is equivalent to the constraints $\|L\|_2 < \sqrt{\kappa_L}$ and $\|Y^{-1}\|_2 < \kappa_Y$, which imply that $\|K\|_2 < \|L\|_2 \|Y^{-1}\|_2 < \sqrt{\kappa_L}\kappa_Y$. Therefore, the stabilization problem under centralized control can be converted to the following optimization problem:

$$
\begin{aligned}
&\min\ c_1\kappa_L + c_2\kappa_Y \\
&\text{subject to} \\
&Y > 0 \\
&YA^T + AY + L^TB^T + BL < 0 \\
&\begin{bmatrix} -\kappa_L I & L^T \\ L & -I \end{bmatrix} < 0 \\
&\begin{bmatrix} Y & I \\ I & \kappa_Y I \end{bmatrix} > 0
\end{aligned}
\tag{5.12}
$$

where the coefficients c_1 and c_2 represent positive weight, reflecting the relative importance of the optimization variables κ_L and κ_Y.

Now let us consider the system stabilization problem under completely decentralized or distributed control. Recall that the problem in (5.12) produces a gain matrix $K = LY^{-1}$. When K_D is a matrix with a nonzero pattern such as block diagonal or an overlapping gain matrix, as shown in Figures 15b and 15c, the problem of finding a distributed control gain can be transformed into the task of searching for matrices L and Y, which are both block diagonal in the case of a completely decentralized structure. Moreover, L has an identical nonzero pattern as that of matrix K_D and Y has a diagonal form in the case of a distributed control structure [73]. When such matrices are denoted as L_D and Y_D, the distributed control design problem takes the following form:

$$
\begin{aligned}
&\min\ c_1\kappa_L + c_2\kappa_Y \\
&\text{subject to} \\
&Y_D > 0 \\
&Y_D A^T + AY_D + L_D^T B^T + BL_D < 0 \\
&\begin{bmatrix} -\kappa_L I & L_D^T \\ L_D & -I \end{bmatrix} < 0 \\
&\begin{bmatrix} Y_D & I \\ I & \kappa_Y I \end{bmatrix} > 0.
\end{aligned} \tag{5.13}
$$

Alternatively, we can follow the procedure proposed in [94] to construct L_D and Y_D in order to achieve distributed control gain with an arbitrary nonzero pattern, where $K_D = L_D Y_D^{-1}$.

5.2 TASK II: FORMULATING AND SOLVING THE SYSTEM STABILIZATION PROBLEM UNDER COMMUNICATION CONSTRAINTS.

For this task, we model the dynamics of communication channels considering both time delays and uncertainties and seek to derive the optimal gain matrix for control under the communication constraints. The aim of this task is to evaluate the performance of various controller structures in stabilizing the power system under communication limitations. By performing this task, we expect to gain insights, valuable in formulating and solving the control structure optimization problem in Task III.

5.2.1 Model Communication Channels

Consider the communication between the two local controllers shown in Figure 16. Without losing generality, consider the channel that delivers the state information of subsystem j,

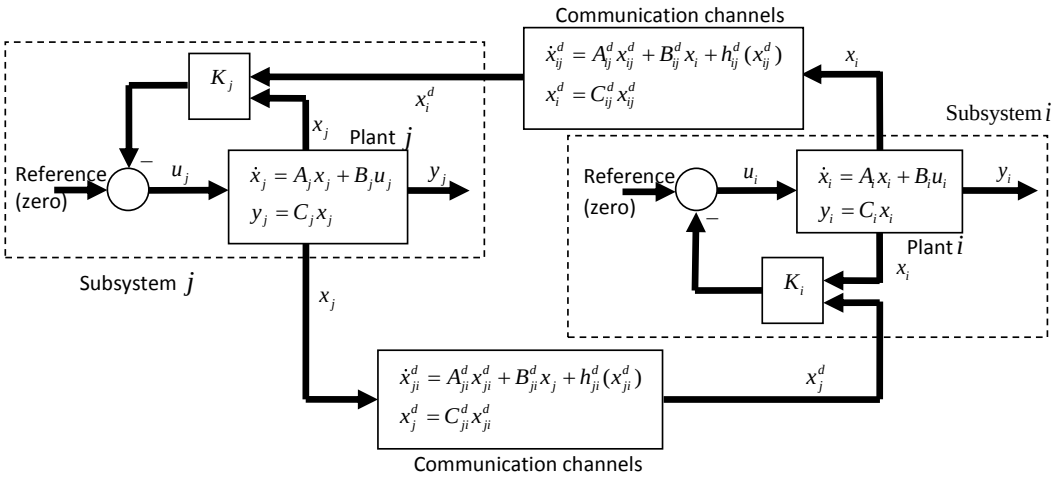

Figure 16: Block diagram of communication channel between subsystems.

i.e., x_j, from the controller of j to that of i. First, the transmission delay in the channel can be modeled by employing a strictly proper rational transfer function, using the Padé approximation [11, 34].The state space equation for the transfer function of the delay is given as

$$\begin{aligned} \dot{x}_{ji}^d &= A_{ji}^d x_{ji}^d + B_{ji}^d x_j \\ x_j^d &= C_{ji}^d x_{ji}^d \end{aligned} \tag{5.14}$$

where x_{ji}^d is the delay state vector, x_j is the controller j state vector and the input vector to the channel, and x_j^d is the channel's output vector to be received at controller i.

Second, the uncertainty, distance, and nonlinearity in the channel can be modeled by a nonlinear function of the state: $h_{ji}^d(x_{ji}^d)$. Therefore, we rewrite (5.14) as the following:

$$\begin{aligned} \dot{x}_{ji}^d &= A_{ji}^d x_{ji}^d + h_{ji}^d(x_{ji}^d) + B_{ji}^d x_j \\ x_j^d &= C_{ji}^d x_{ji}^d. \end{aligned} \tag{5.15}$$

Through the communication channels, controller i can collect the state information from the other nodes j and use this information to calculate the control signal according to the following:

$$u_i = K_{ii}x_i + \sum_{i \neq j} K_{ij}x_j^d \equiv K_i \bar{x}_i \tag{5.16}$$

where K_{ii} and x_i are the gain matrix and the state vector for local controller i, respectively. K_{ij} is the gain matrix assigned to the state information (x_j^d) which is sent from node j. K_i and $\bar{x}_i$ are symbols introduced to simplify the expressions:

$$\bar{x}_i = \left[\underbrace{(x_1^d)^T, \cdots, (x_j^d)^T, \cdots, (x_{i-1}^d)^T}_{1 \leq j < i}, (x_i)^T, \underbrace{(x_{i+1}^d)^T, \cdots, (x_j^d)^T, \cdots, (x_N^d)^T}_{i < j \leq N} \right]^T \tag{5.17}$$

$$K_i = \left[\underbrace{K_{i,1}, \cdots, K_{i,j}, \cdots, K_{i,i-1}}_{1 \leq j < i}, K_i, \underbrace{K_{i,i+1}, \cdots, K_{i,j}, \cdots, K_{i,N}}_{i < j \leq N} \right] \tag{5.18}$$

5.2.2 Model of Augmented System

We now combine the dynamics of the power system and those of the communication channels to form an augmented system:

$$\dot{\bar{x}} = (\bar{A} + \bar{B}\bar{K}_D)\bar{x} + h(\bar{x}). \tag{5.19}$$

In the above equation, $\bar{x}$ is the augmented state vector, defining $\bar{x} = [\bar{x}_1^T, \bar{x}_2^T, \cdots, \bar{x}_N^T]$, where each $\bar{x}_i$ is defined by (5.17) and (5.15); $\bar{A}$, $\bar{B}$, and $\bar{K}_D$ can be derived from (5.2), along with (5.14)-(5.18). $\bar{K}_D$ depends linearly on the elements of K_D, which characterize the interconnection topology of the controllers; $h(\bar{x})$ summarizes the unmolded nonlinearities or uncertainties of the power system and communication channels.

5.2.3 Stabilization Problem

Consider the system stabilization problem under the communication constraints and the controller interconnection topology characterized by the nonzero patterns of matrix $\bar{K}_D$. Equation (5.19) contains the nonlinear term $h(\bar{x})$. In order to simplify the analysis, we consider a specific, yet sufficiently general class of functions which satisfies the inequality

$$h^T(\bar{x})h(\bar{x}) \leq \alpha^2 \bar{x}^T H^T H \bar{x} \tag{5.20}$$

where H is a constant square matrix of dimension, and α is a scalar parameter. Here α can be viewed as a measure of robustness with respect to uncertainties. One objective in this procedure is to maximize such robustness, or α, by choosing the appropriate control gain $\bar{K}_D$.

With respect to $h(\bar{x})$ and inequality (5.20), system (5.19) is globally asymptotically stable if we can find a control gain $\bar{K}_D$, symmetric matrix $P > 0$, and scalar $\tau > 0$ such that

$$\begin{bmatrix} (\bar{A} + \bar{B}\bar{K}_D)^T P + P(\bar{A} + \bar{B}\bar{K}_D) + \tau\alpha^2 H^T H & P \\ P & -\tau I \end{bmatrix} < 0. \tag{5.21}$$

Introducing matrices Y_D, L_D, and positive scalar γ defined by the equations

$$Y_D = \tau P^{-1}, L_D = \bar{K}_D Y_D, \text{ and } \gamma = 1/\alpha^2. \tag{5.22}$$

We can use the Schur complement formulation [39] to express (5.21) as

$$\begin{bmatrix} Y_D\bar{A}^T + \bar{A}Y_D + L_D^T\bar{B}^T + \bar{B}L_D & I & Y_D H^T \\ I & -I & 0 \\ HY_D & 0 & -\gamma I \end{bmatrix} < 0 \tag{5.23}$$

Moreover, by following the same procedure as used in (5.11) to bound $\bar{K}_D$, in (5.23) the stabilization optimization problem becomes

$$
\begin{aligned}
&\min\ c_1\kappa_L + c_2\kappa_Y + c_3\gamma \\
&Y_D > 0 \\
&\begin{bmatrix} Y_D\bar{A}^T + \bar{A}Y_D + L_D^T\bar{B}^T + \bar{B}L_D & I & Y_DH^T \\ I & -I & 0 \\ HY_D & 0 & -\gamma I \end{bmatrix} < 0 \\
&\begin{bmatrix} -\kappa_L I & L_D^T \\ L_D & -I \end{bmatrix} < 0 \\
&\begin{bmatrix} Y_D & I \\ I & \kappa_Y I \end{bmatrix} > 0
\end{aligned}
\tag{5.24}
$$

where the coefficients c_1, c_2, and c_3 represent positive weights reflecting the relative importance of the optimization variables κ_L , κ_L , and γ . If the LMI optimization is feasible, the resulting gain matrix stabilizes the close loop system for all nonlinearities or uncertainties which satisfy (5.20).

5.3 TASK III: FORMULATING AND SOLVING THE STRUCTURAL OPTIMIZATION PROBLEM FOR CONTROL STRUCTURE SYNTHESIS

Having completed the preparation, consisting of Tasks I and II, we can formulate the controller structure synthesis problem, the goal of which is to find the optimal topology of the distributed controller in Figure 8. This structure minimization or optimization problem integrates concerns with communication complexity in the design of the control system.

5.3.1 Structural Optimization Problem

The main design innovation in this thesis is to include in the cost function a term that punishes communication complexity in controller interconnection topology. Note that communication complexity can be reflected in the number of channels established to exchange information between controllers. In other words, the complexity of communication is closely related to the sparsity or nonzero pattern of the control gain matrix $\bar{K}_D$. A sparser matrix $\bar{K}_D$ corresponds to a network control topology with fewer demands on its communication capacity. Therefore, we can use the number of nonzero elements in $\bar{K}_D$ to quantify communication complexity. Whenever the system performance permits, we prefer to use a sparser $\bar{K}_D$ to reduce the dimensionality in control and communication.

It should be noted that $\bar{K}_D$ does not appear explicitly in the system stabilization problem (5.24), but is computed through L_D and Y_D (where $\bar{K}_D = L_D Y_D^{-1}$). Matrix L_D has a nonzero pattern identical to that of matrix $\bar{K}_D$ [73]. Therefore, the problem becomes one of finding a sparser L_D to reduce the communication complexity and dimensionality in the control, in order to find the optimal topology.

Formally, we want to add to the cost function of (5.24) a punishment term $c_4\|L_D\|_0$, where $\|L_D\|_0$ denotes the number of nonzero elements in L_D, while c_4 is a positive weight reflecting how desirable it is to reduce the communication complexity. In general, the resulting optimization problem is difficult to solve, because it requires enumerating the nonzero patterns of L_D. The computational complexity of this procedure grows exponentially with the dimensions of L_D [32]. Instead of minimizing $c_4\|L_D\|_0$ directly, we can consider an approximation of it using ℓ_1-minimization. In order to do this, we replace $\|L_D\|_0$ with $\sum_i \sum_j |L_{ij}|$, the sum of the absolute values of all elements of L_D, where L_{ij} denotes the element on the i'th row and the j'th column of matrix. Use of the ℓ_1- minimization problem to minimize $\sum_i \sum_j |L_{ij}|$ can be considered to be a type of convexification of the problem of minimizing $\|L_D\|_0$: the former is the closest convex optimization problem to the latter L_D [32]. An added benefit of using ℓ_1-minimization is that it can produce a sparse solution [78].

Base on the above arguments, we formulate the structure optimization problem as

$$
\begin{aligned}
&\min\ c_1\kappa_L + c_2\kappa_Y + c_3\gamma + c_4 \sum_i \sum_j |L_{ij}| \\
&Y_D > 0 \\
&\begin{bmatrix} Y_D\bar{A}^T + \bar{A}Y_D + L_D^T\bar{B}^T + \bar{B}L_D & I & Y_DH^T \\ I & -I & 0 \\ HY_D & 0 & -\gamma I \end{bmatrix} < 0 \\
&\begin{bmatrix} -\kappa_L I & L_D^T \\ L_D & -I \end{bmatrix} < 0 \\
&\begin{bmatrix} Y_D & I \\ I & \kappa_Y I \end{bmatrix} > 0
\end{aligned}
\tag{5.25}
$$

where the coefficients c_1, c_2, c_3, and c_4 represent positive weights reflecting the relative importance of the terms in the cost function. The above problem can be solved efficiently using standard optimization techniques for LMI optimization and ℓ_1- minimization.

5.3.2 Role of the Central Controller in the Hierarchy

The central controller is located in the top layer of the hierarchical control architecture as shown in Figure 8. Its role is to coordinate the operations of the local controllers in the decentralized control layer: to accomplish this, it adaptively optimizes and updates the control and communication topology in real time.

5.4 DESIGN OF OPTIMAL STRUCTURE

Step 1: Design decision matrix Y_D as a block diagonal matrix and decision matrix L_D as a full dimension matrix.

Step 2: Insert Y_D and L_D decision matrices into the structure optimization problem (5.25).

$$\min\ c_1\kappa_L + c_2\kappa_Y + c_3\gamma + c_4 \sum_i \sum_j |L_{ij}|$$

$$Y_D > 0$$

$$\begin{bmatrix} Y_D\bar{A}^T + \bar{A}Y_D + L_D^T\bar{B}^T + \bar{B}L_D & I & Y_DH^T \\ I & -I & 0 \\ HY_D & 0 & -\gamma I \end{bmatrix} < 0$$

$$\begin{bmatrix} -\kappa_L I & L_D^T \\ L_D & -I \end{bmatrix} < 0$$

$$\begin{bmatrix} Y_D & I \\ I & \kappa_Y I \end{bmatrix} > 0$$

Step 3: Compute $K_D = L_D Y_D^{-1}$.

Step 4:

(a) for $i = 1 : \ldots : M$, where M is the total number of feedback gain with sharing state variables.

(b) obtain the $K_D(i)$ structure.

(c) redesign decision matrix $L_D(i)$ to have the same matrix structure as as $K_D(i)$, redesign decision matrix $Y_D(i)$ as a block diagonal matrix.

(d) insert decision matrices $Y_D(i)$ and $L_D(i)$ into the fixed structure optimization problem (5.24).

$$\min\ c_1\kappa_L + c_2\kappa_Y + c_3\gamma$$

$$Y_D > 0$$

$$\begin{bmatrix} Y_D\bar{A}^T + \bar{A}Y_D + L_D^T\bar{B}^T + \bar{B}L_D & I & Y_DH^T \\ I & -I & 0 \\ HY_D & 0 & -\gamma I \end{bmatrix} < 0$$

$$\begin{bmatrix} -\kappa_L I & L_D^T \\ L_D & -I \end{bmatrix} < 0$$

$$\begin{bmatrix} Y_D & I \\ I & \kappa_Y I \end{bmatrix} > 0$$

(e) compute $K_D(i) = L_D(i)Y_D^{-1}(i)$.

(f) calculate the energy cost, then go to Step 4(a).

Step 5: The optimal topology of distributed control is the $K_D(i)$ structure with minimum energy cost $J(i)$.

5.5 DEMONSTRATION OF CONTROL DESIGN METHODS

In this task, we demonstrate on a test-bed the hierarchical control architecture and controller-structure design methods developed in three tasks. The goal of the control system is to suppress of the inter-area low-frequency oscillations. Communication constraints are used to compare the performance of our design with those of the conventional designs and centralized control design under communication constraints. For this thesis, we demonstrate our control design methods on an IEEE 39-bus power system.

The IEEE 39-bus power system includes 10 generators, 29 loads, and 40 transmission lines, as shown in Figure 17. The power system is modeled as shown in Section 4.1.1. The performance of the control system synthesized by our method will be evaluated by the

eigenvalues and the damping ratio of the open-loop and closed-loop systems and through nonlinear simulations. For comparison purposes, we have run both a completely decentralized and an entirely centralized design in our system modeling, including in our design both time delays and communication uncertainties.

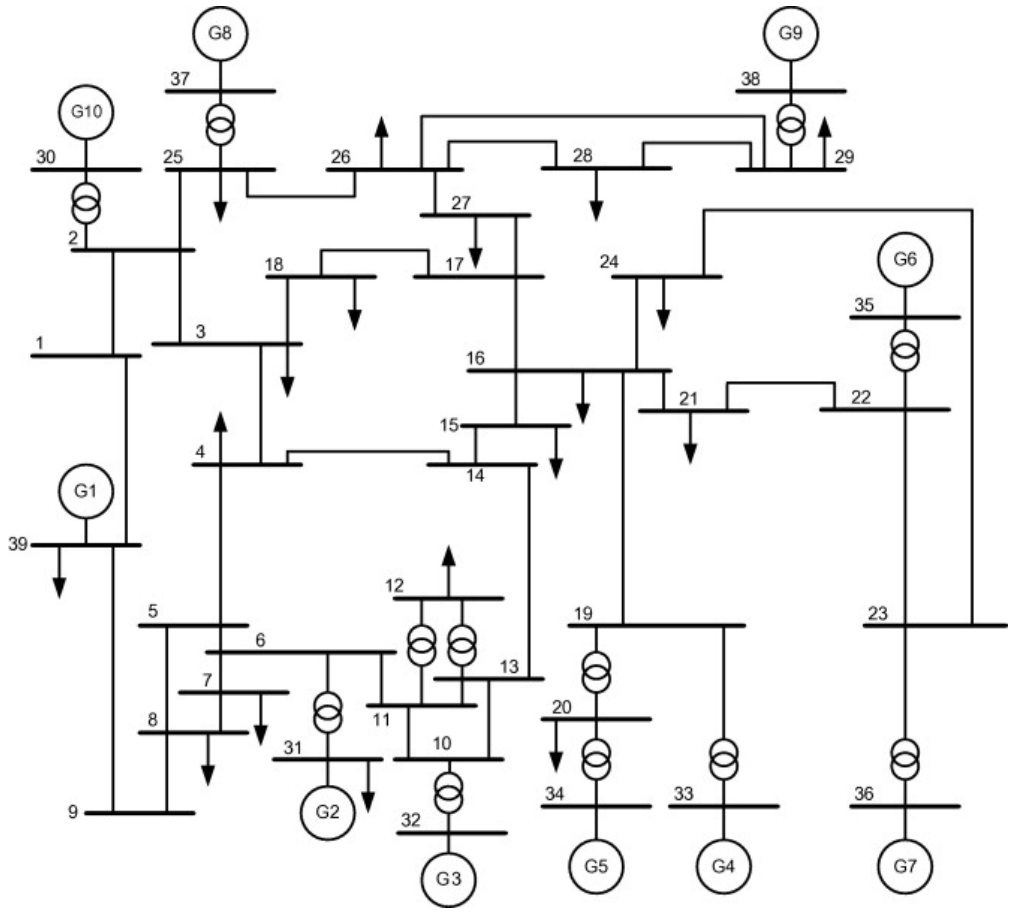

Figure 17: IEEE 39-bus power system (figure adapted from [1]).

6.0 SIMULATION RESULTS AND DISCUSSION

6.1 SIMULATION RESULTS

In this section, we have applied our hierarchical control architecture and controller structure design methods developed in Tasks I, II, and III on an IEEE 39-bus power system as shown in Figure 17, with the goal to design a control system that suppresses inter-area low-frequency oscillations. In our design, we consider communication constraints.

6.1.1 Power System Description

The IEEE 39-bus power system includes 10 generators, 29 loads, and 40 transmission lines. For purpose of this study, this system was partitioned into ten control areas, with one generator in each area, as shown in Figure 18. The structure of decomposition and the connected tie-lines for the ten areas are shown in Table 1. The tie-line topology between areas was selected arbitrarily. The generator, turbine, and governor parameters are shown in Table 2. The line parameters are given in Table 3. The load flow solution [97] for the voltages and angles of the buses are shown in Table 4. Table 5 provides the synchronizing torques of the tie-lines, which were calculated based on a power flow analysis of the IEEE 39-bus power system using Equation 4.18.

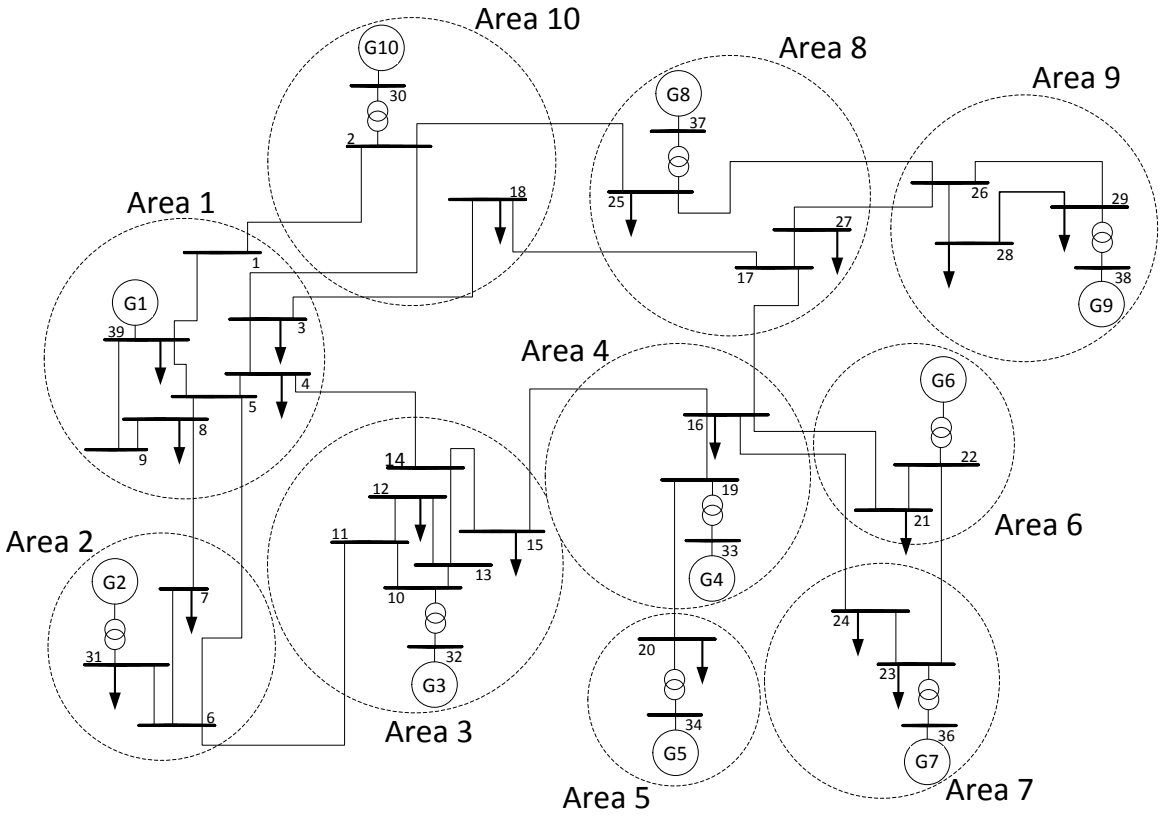

Figure 18: IEEE 39-bus power system decomposed into ten control areas.

Table 1: Decomposition of the IEEE 39-bus power system.

Area	**Generator**	**Buses**	**Connected to Area**	**Connected tie-line**
1	G1	1, 3, 4, 5,	2	7-8
		8, 9, 39	3	4-14
			10	1-2, 2-3, 3-18
2	G2	6, 7, 31	1	7-8
			3	6-11
3	G3	10, 11, 12, 13,	1	4-14
		14, 15	2	6-11
			4	15-16
4	G4	16, 19, 33	3	15-16
			5	19-20
			6	16-21
			7	16-24
			8	16-17
5	G5	20, 34	4	19-20
6	G6	21, 22	4	15-16
			7	22-23
7	G7	23, 24, 36	4	16-24
			6	22-23
8	G8	17, 25, 27, 37	4	16-17
			9	26-27
			10	17-18, 2-25
9	G9	26, 28, 29, 38	8	26-27
10	G10	2, 18, 30	1	1-2, 2-3, 3-18
			8	17-18, 2-25

Table 2: Generator, turbine, and governor parameters for the IEEE 39-bus system (per unit).

Generator	$\boldsymbol{M}$	$\boldsymbol{D}$	$\boldsymbol{T_{ch}}$	$\boldsymbol{T_g}$	$\boldsymbol{R}$
1	6.0	5.0	0.20	0.25	0.05
2	3.0	4.0	0.20	0.25	0.05
3	2.5	4.0	0.20	0.25	0.05
4	4.0	6.0	0.20	0.25	0.05
5	2.0	3.5	0.20	0.25	0.05
6	3.5	3.0	0.20	0.25	0.05
7	3.0	7.5	0.20	0.25	0.05
8	2.5	4.0	0.20	0.25	0.05
9	2.0	6.5	0.20	0.25	0.05
10	4.0	5.0	0.20	0.25	0.05

Table 3: Line parameters for the IEEE 39-bus power system (per unit).

Line	1-2	1-39	2-3	2-25	2-30	3-4	3-18	4-5
$\boldsymbol{r}$	0.0035	0.0020	0.0013	0.0070	0.0000	0.0013	0.0011	0.0008
$\boldsymbol{x}$	0.0411	0.0500	0.0151	0.0086	0.0181	0.0213	0.0133	0.0128
Line	4-14	5-6	5-8	6-7	6-11	6-31	7-8	8-9
$\boldsymbol{r}$	0.0008	0.0002	0.0008	0.0006	0.0007	0.0000	0.0004	0.0023
$\boldsymbol{x}$	0.0129	0.0026	0.0112	0.0092	0.0082	0.0500	0.0046	0.0363
Line	9-39	10-11	10-13	10-32	12-11	12-13	13-14	14-15
$\boldsymbol{r}$	0.0010	0.0004	0.0004	0.0000	0.0016	0.0016	0.0009	0.0018
$\boldsymbol{x}$	0.0250	0.0043	0.0043	0.0200	0.0435	0.0435	0.0101	0.0217
Line	15-16	16-17	16-19	16-21	16-24	17-18	17-27	19-20
$\boldsymbol{r}$	0.0009	0.0007	0.0016	0.0008	0.0003	0.0007	0.0013	0.0007
$\boldsymbol{x}$	0.0094	0.0089	0.0195	0.0135	0.0059	0.0082	0.0173	0.0138
Line	19-33	20-34	21-22	22-23	22-35	23-24	23-36	25-26
$\boldsymbol{r}$	0.0007	0.0009	0.0008	0.0006	0.0000	0.0022	0.0005	0.0032
$\boldsymbol{x}$	0.0142	0.0180	0.0140	0.0096	0.0143	0.0350	0.0272	0.0323
Line	25-37	26-27	26-28	26-29	28-29	29-38		
$\boldsymbol{r}$	0.0006	0.0014	0.0043	0.0057	0.0014	0.0008		
$\boldsymbol{x}$	0.0232	0.0147	0.0474	0.0625	0.0151	0.0156		

Table 4: Voltage and angle parameters for the IEEE 39-bus power system (per unit).

Bus	1	2	3	4	5	6	7	8
$\boldsymbol{V}$	1.0163	0.9979	0.9616	0.9267	0.9299	0.9327	0.9223	0.9223
$\boldsymbol{\delta}$	-0.1779	-0.1269	-0.1811	-0.1959	-0.1709	-0.1565	-0.2015	-0.2119
Bus	9	10	11	12	13	14	15	16
$\boldsymbol{V}$	0.9861	0.9421	0.9372	0.9165	0.9377	0.9334	0.9393	0.9606
$\boldsymbol{\delta}$	-0.2097	-0.1083	-0.1247	-0.1251	-0.1229	-0.1572	-0.1668	-0.1390
Bus	17	18	19	20	21	22	23	24
$\boldsymbol{V}$	0.9584	0.9572	0.9795	0.9808	0.9721	1.0075	1.0052	0.9697
$\boldsymbol{\delta}$	-0.1590	-0.1760	-0.0461	-0.0713	-0.0921	-0.0073	-0.0114	-0.1368
Bus	25	26	27	28	29	30	31	32
$\boldsymbol{V}$	1.0059	0.9725	0.9571	0.9817	0.9940	1.0475	0.9820	0.9831
$\boldsymbol{\delta}$	-0.0997	-0.1213	-0.1620	-0.0517	0.0015	-0.0836	0	0.0325
Bus	33	34	35	36	37	38	39	
$\boldsymbol{V}$	0.9972	1.0123	1.0493	1.0635	1.0278	1.0265	1.0300	
$\boldsymbol{\delta}$	0.0451	0.0194	0.0807	0.1304	0.0211	0.1270	-0.2074	

Table 5: Synchronizing torque coefficient between the buses (per unit).

Line	1-2	1-39	2-3	2-25	2-30	3-4	3-18
$\boldsymbol{T_{ij}}$	24.6435	20.9267	63.4551	116.6763	57.6973	41.8318	69.2054
Line	4-5	4-14	5-6	5-8	6-7	6-11	6-31
$\boldsymbol{T_{ij}}$	67.3023	67.0026	333.5492	76.5113	93.4085	106.5469	18.0944
Line	7-8	8-9	9-39	10-11	10-13	10-32	12-11
$\boldsymbol{T_{ij}}$	184.9111	25.0545	40.6272	205.3064	205.4216	45.8507	19.7458
Line	12-13	13-14	14-15	15-16	16-17	16-19	16-21
$\boldsymbol{T_{ij}}$	19.7563	86.6074	40.4010	95.9514	103.4219	48.0436	69.0943
Line	16-24	17-18	17-27	19-20	19-33	20-34	21-22
$\boldsymbol{T_{ij}}$	157.9292	111.8595	53.0220	69.5934	68.4999	54.9324	69.7051
Line	22-23	22-35	23-24	23-36	25-26	25-37	26-27
$\boldsymbol{T_{ij}}$	105.4928	73.6419	27.6311	38.9081	30.2789	44.2384	63.2659
Line	26-28	26-29	28-29	29-38			
$\boldsymbol{T_{ij}}$	20.0927	15.3502	64.5317	64.8921			

6.1.2 Open-loop System Analysis

Before designing the distributed control of the power system, we have shown the eigenvalues of the open-loop system. Examining the eigenvalues of the open-loop system (5.1) under a centralized structure, we note that there are some poles in the open right half plane. The poles with positive values are shown in Figure 19. Therefore, the system is unstable.

In such an unstable system, once any area of the power system faces a small disturbance, inter-area oscillations may result. Assuming that the power system is operating at a steady state condition, we create non-zero initial frequency state conditions in Area 4 and Area 8, which may be caused by the changing load in these areas. Figure 20 shows the system response of the open-loop system to a non-zero initial frequency occurring in Areas 4 and

8. Should this occur, every generator increases or decreases power in order to meet the increasing or decreasing demand of the load. It is clear that small disturbances in two areas cause a change in frequency in all areas; moreover, the frequencies cannot return to a steady state. This leads to a swing of the generator in each area against generators in other areas.

Such a small signal disturbance in an uncontrolled system could cause the system to experience inter-area low-frequency oscillations. This may cause serious problems that can lead to wide spread blackouts in the power system. Therefore, the goal of our control method is to design a topology of distributed control for the power system to ensure global asymptotic stability.

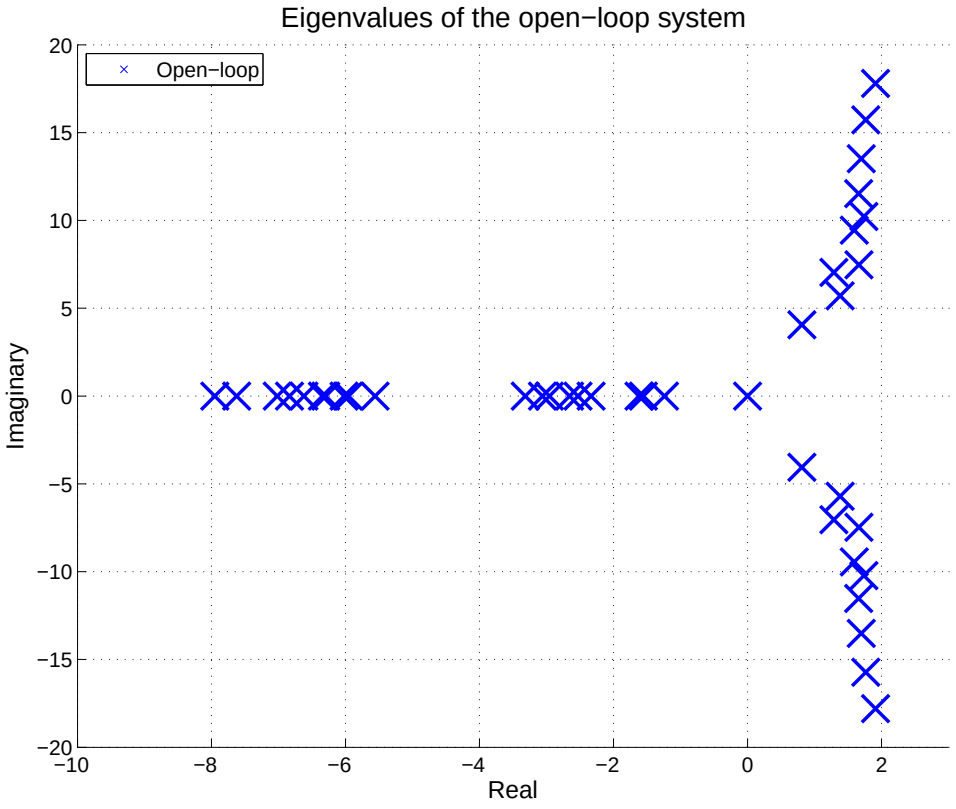

Figure 19: Eigenvalues of the open-loop system.

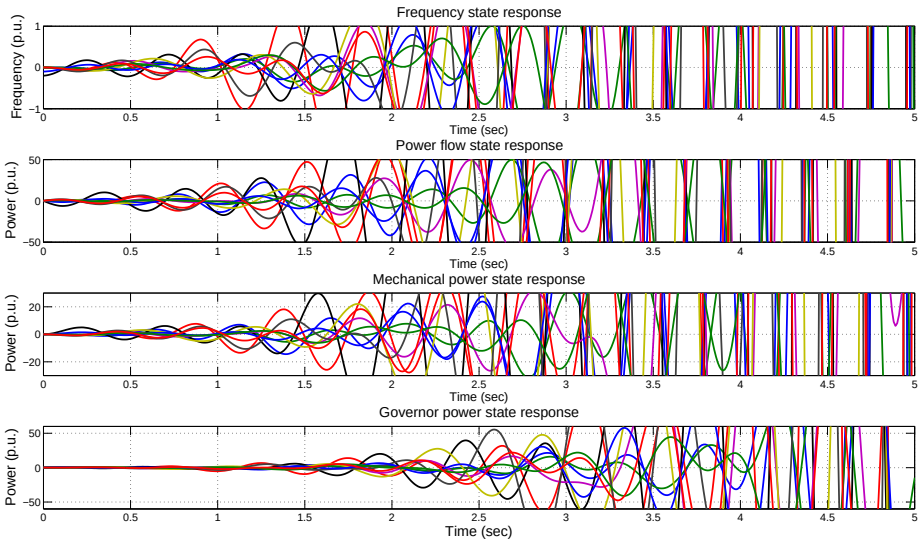

Figure 20: Open-loop system response to a non-zero initial condition in Areas 4 and 8.

6.1.3 Designing Distributed Control

In this section, we show the steps we have taken to find the optimal topology of distributed control for the ten areas chosen for the simulation. All the simulations in this thesis were completed using the MATLAB toolbox from [60] and [86].

Step 1: As mentioned earlier, K_D does not appear explicitly in the system stabilization problem (5.25), but it is computed through L_D and Y_D. Therefore, the first step was to design the decision matrix Y_D as a block diagonal matrix and a decision matrix L_D as a full dimension matrix, both of which are shown in Figure 21. Each small square represents a subsystem (one area). In the L_D matrix, each small colored square signifies that each subsystem (area) is allowed to communicate with other subsystems (areas) only through their shared state variables. Making L_D a full dimension matrix that each controller has the opportunity to establish communication with all other controllers.

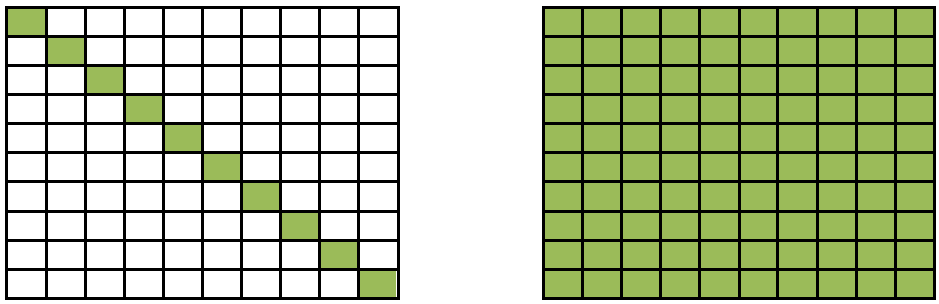

Figure 21: (a) The structure of the diagonal decision matrix Y_D. (b) The structure of the full dimension decision matrix L_D.

Step 2: We inserted decision matrices Y_D and L_D into the structure optimization problem (5.25), and then exported the solution matrices Y_D and L_D as shown in Figure 22.

$$
\begin{aligned}
&\min\ c_1\kappa_L + c_2\kappa_Y + c_3\gamma + c_4 \sum_i \sum_j |L_{ij}| \\
&Y_D > 0 \\
&\begin{bmatrix} Y_D\bar{A}^T + \bar{A}Y_D + L_D^T\bar{B}^T + \bar{B}L_D & I & Y_D H^T \\ I & -I & 0 \\ HY_D & 0 & -\gamma I \end{bmatrix} < 0 \\
&\begin{bmatrix} -\kappa_L I & L_D^T \\ L_D & -I \end{bmatrix} < 0 \\
&\begin{bmatrix} Y_D & I \\ I & \kappa_Y I \end{bmatrix} > 0
\end{aligned}
$$

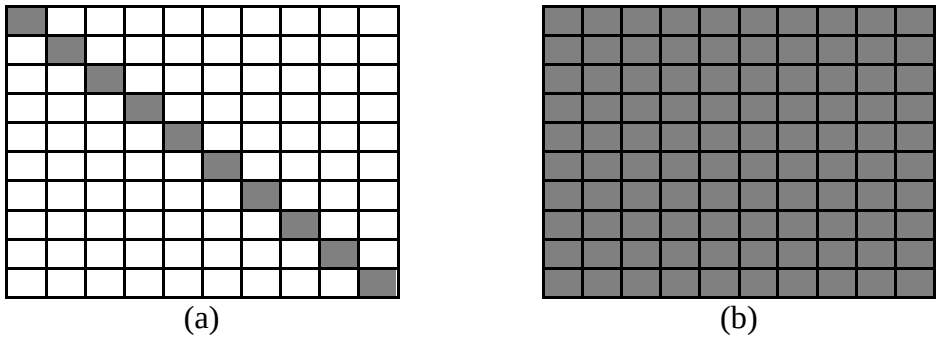

Figure 22: (a) Y_D solution matrix. (b) L_D solution matrix.

Step 3: We computed the K_D matrix such that $K_D = L_D Y_D^{-1}$. Because the L_D matrix was designed as a full dimension matrix, the K_D matrix was also expected to be a full dimension matrix as shown in Figure 23. This K_D matrix, as a locally centralized structure, allows each controller communicate with all other controllers. However, because of the ℓ_1-minimization of L_D in the cost function of the optimization problem, this K_D matrix provides valuable information about the weaknesses and strengths of the feedback gain values. These weaknesses and strengths can in turn be represented as the weaknesses and strengths of the communication between controllers. Figure 24 shows these feedback gain values for each of four state variables. Approximately two thirds of the feedback gain values are near to zero, which may be considered non-communication.

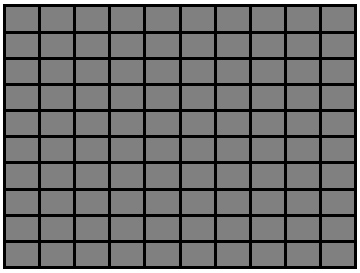

Figure 23: K_D solution matrix resulting from step 2.

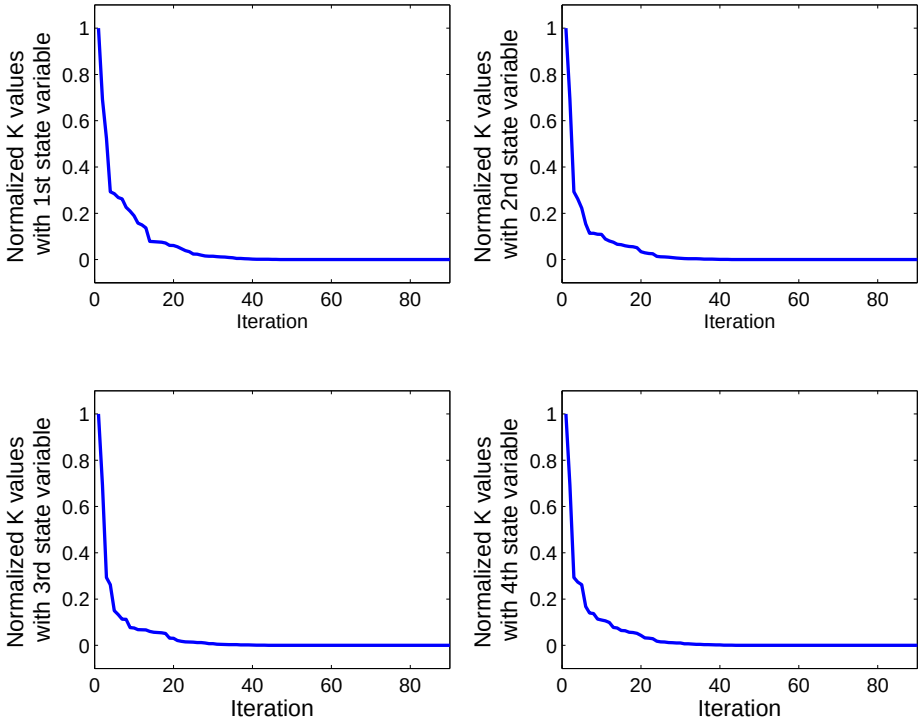

Figure 24: Feedback gain values in the K_D matrix.

Step 4: We identified the communication channels necessary to stabilize the global system at the minimum energy cost, by applying following loop.

(a) for $i = 1, \ldots, M$, where M is the total number of feedback gain values with each state variable.

(b) obtain the $K_D(i)$ structure, as shown in Figure 25.

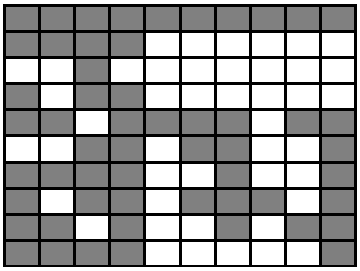

Figure 25: Example of a fixed $K_D(i)$ matrix structure.

(c) redesign the decision matrix $L_D(i)$ to be identical to the $K_D(i)$ matrix structure; redesign the decision matrix $Y_D(i)$ as a block diagonal matrix.

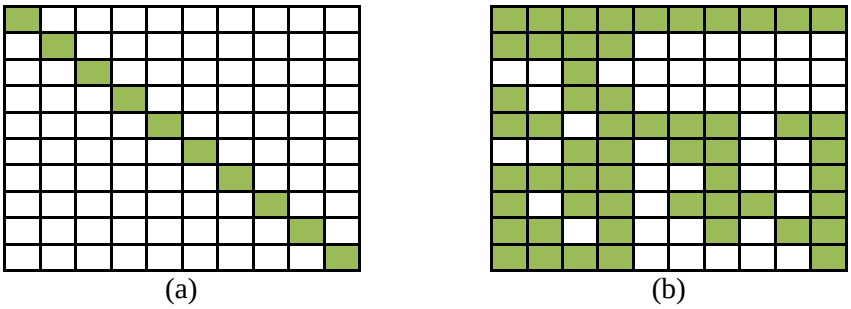

Figure 26: (a) Example of the structure of the diagonal decision matrix Y_D(i). (b) Example of the fixed structure of decision matrix L_D(i).

(d) now that the $Y_D(i)$ and $L_D(i)$ matrices have a fixed structure, insert decision matrices $Y_D(i)$ and $L_D(i)$ into the fixed structure optimization problem (5.24).

$$\min\ c_1\kappa_L + c_2\kappa_Y + c_3\gamma$$

$$Y_D > 0$$

$$\begin{bmatrix} Y_D\bar{A}^T + \bar{A}Y_D + L_D^T\bar{B}^T + \bar{B}L_D & I & Y_DH^T \\ I & -I & 0 \\ HY_D & 0 & -\gamma I \end{bmatrix} < 0$$

$$\begin{bmatrix} -\kappa_L I & L_D^T \\ L_D & -I \end{bmatrix} < 0$$

$$\begin{bmatrix} Y_D & I \\ I & \kappa_Y I \end{bmatrix} > 0$$

(e) compute the K_D matrix such that $K_D = L_D Y_D^{-1}$, as shown in Figure 27.

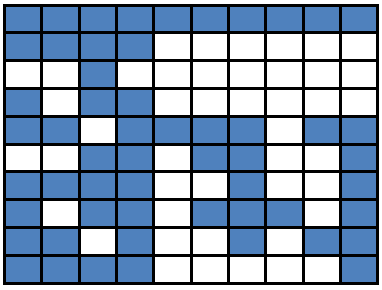

Figure 27: $K_D(i)$ matrix structure with actual feedback gain values.

(f) calculate energy cost, then go Step 4(a).

Step 5: We identify the optimal structure as the $K_D(i)$ structure with the minimum energy cost. Figure 28 shows the increment of dimension for each controller. Faster increment dimensions indicate that these controllers are essential to establishing communication with some of the correlated controllers. For instance, Controllers 1, 2 and 7 are the controllers most needed to begin communication with other controllers. On the other hand, Controllers 3 and 4 are less necessary for establishing communication with other controllers.

Figure 29 illustrates the relationship between the total control dimension, the damping

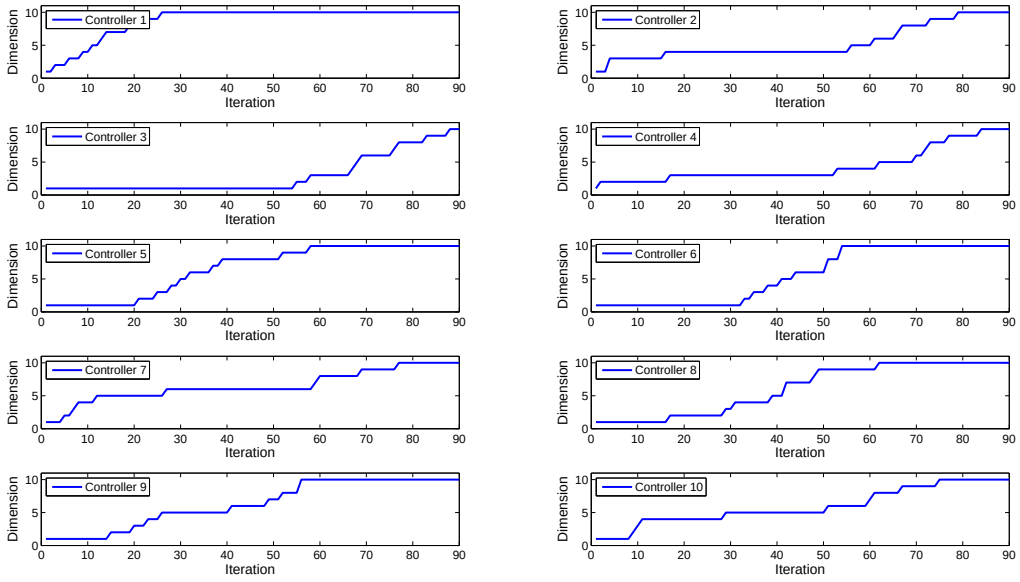

Figure 28: The variation in the dimensions of each of the ten controllers.

ratio, and the energy cost from Step 4. After considering these relationships, we assert that increasing the number of communication channels clearly does not translate into better energy cost. On the other hand, including unnecessary communication channels or ignoring essential channels in order to stabilize the system may result in a very high energy cost, as shown in Figure 29. It further appears to be clear that improving the damping ratio can help avoid putting the system at risk of inter-area oscillations. The optimal structure, then, is based on manipulating the relationship between the dimension, the damping ratio, and the energy cost. Consequently, in this simulation, J(i) at $i = 20$ has the minimum energy cost for

the design of a feedback state control of this system. At the same time, the K(i) structure at $i = 20$ is the optimal structure for distributed control with a high damping ratio, as shown in Figure 30. The arrangement of the communication channels designed to connect controllers is shown in Figure 31. Controller 1 receives state information from Controllers 3-5 and 7-10. Controllers 1, 3, and 4 send their state variables to Controller 2. Controller 4 would receive state information from Controllers 1 and 3 and so forth, for the other controllers.

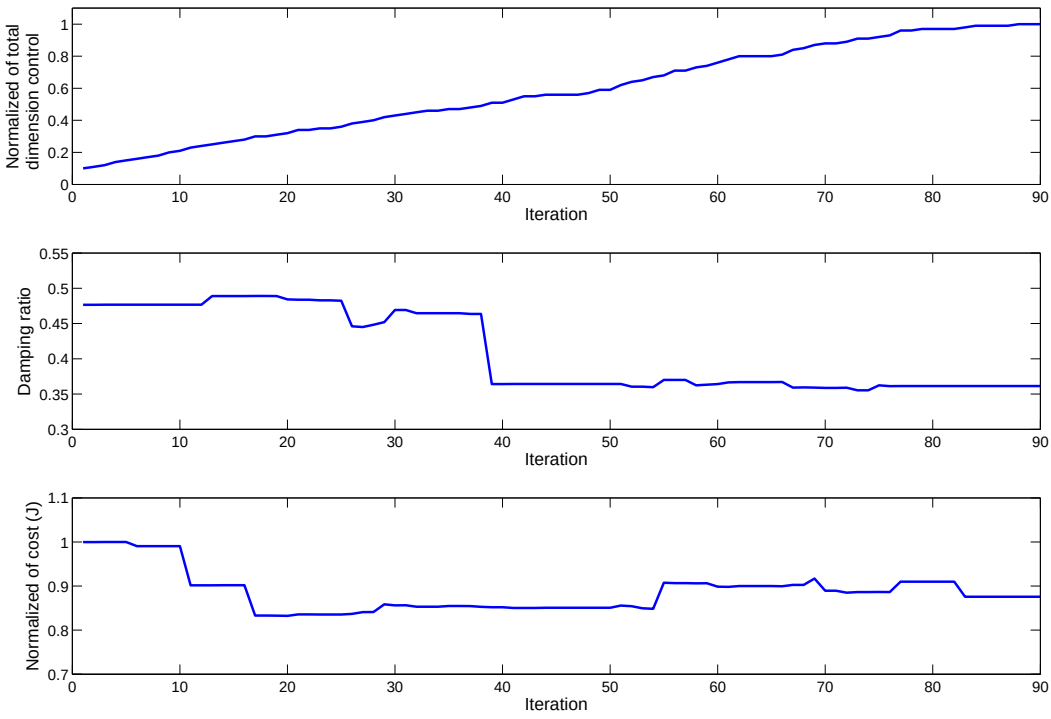

Figure 29: The relationship between total control dimension, damping ratio, and energy cost.

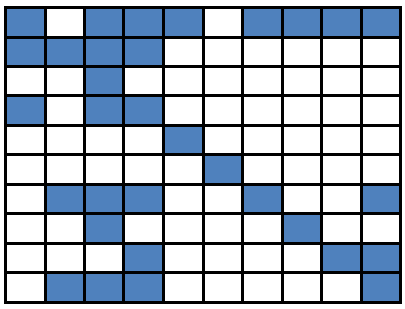

Figure 30: Optimal feedback gain structure of distributed control.

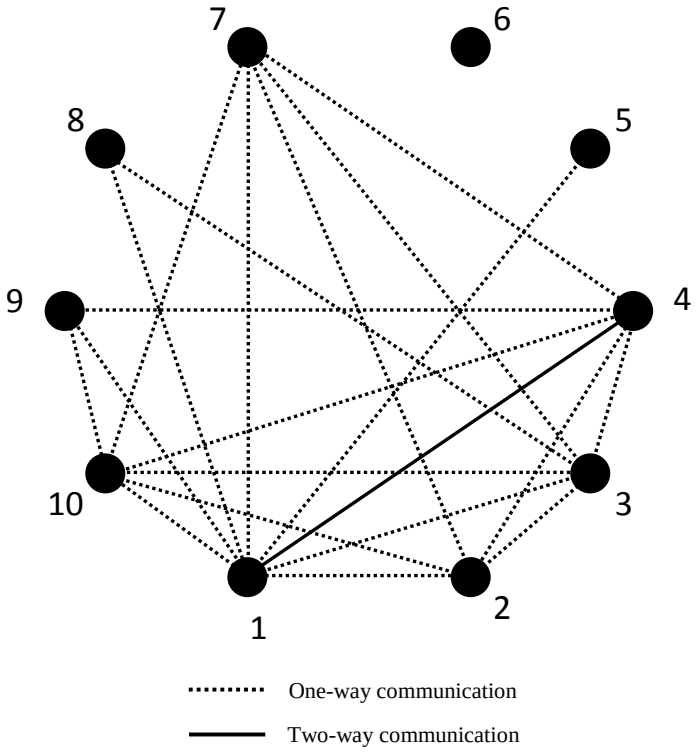

Figure 31: Communication channels assigned among the ten controllers.

6.1.4 Optimal Design Simulation

In Figure 32 we can see that all eigenvalues of the closed-loop (optimal structure) system are on the left side of the imaginary axis of the complex plan. Therefore, the system is stable. Furthermore, as shown in Table 6, all damping ratios corresponding to the eigenvalues are above the critical ratio. In order to validate our design, we created non-zero initial frequency state conditions in Areas 4 and 8, which was caused by changing of the load in these areas. The optimal design successfully returned all states to a zero steady state after two seconds, as shown in Figure 33. The other states in the other controller areas were not influenced by the non-zero initial frequency state conditions. Based on the optimal structure solution, we can write the control law for each controller, as shown in Table 7.

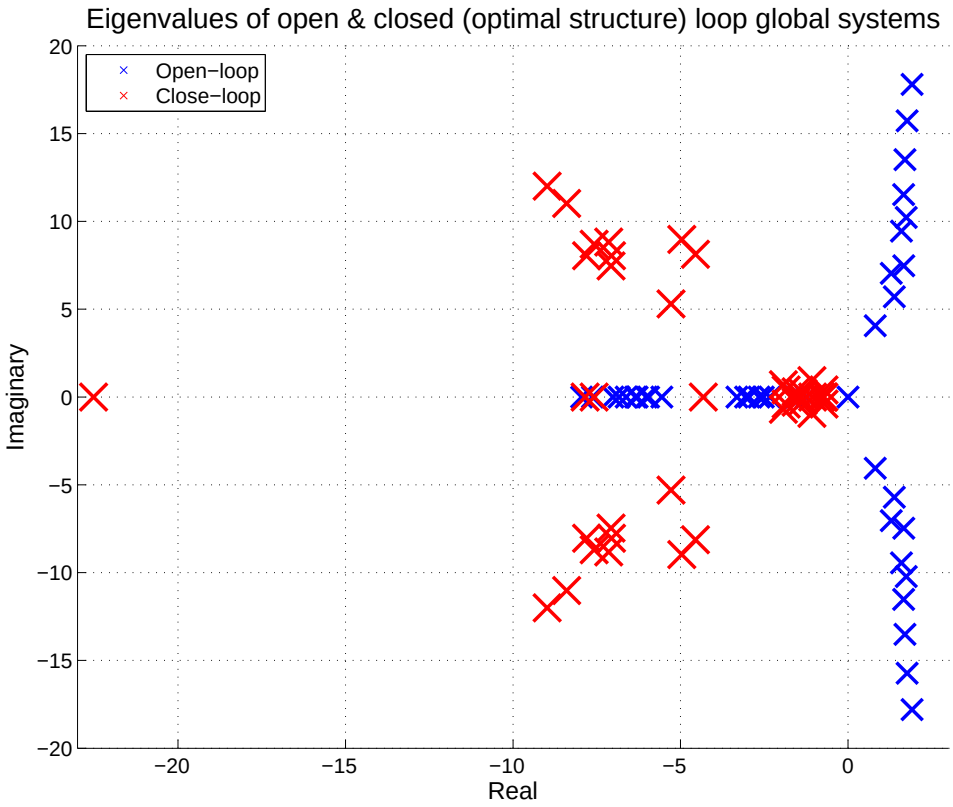

Figure 32: Eigenvalues of open and closed (optimal structure) loop system.

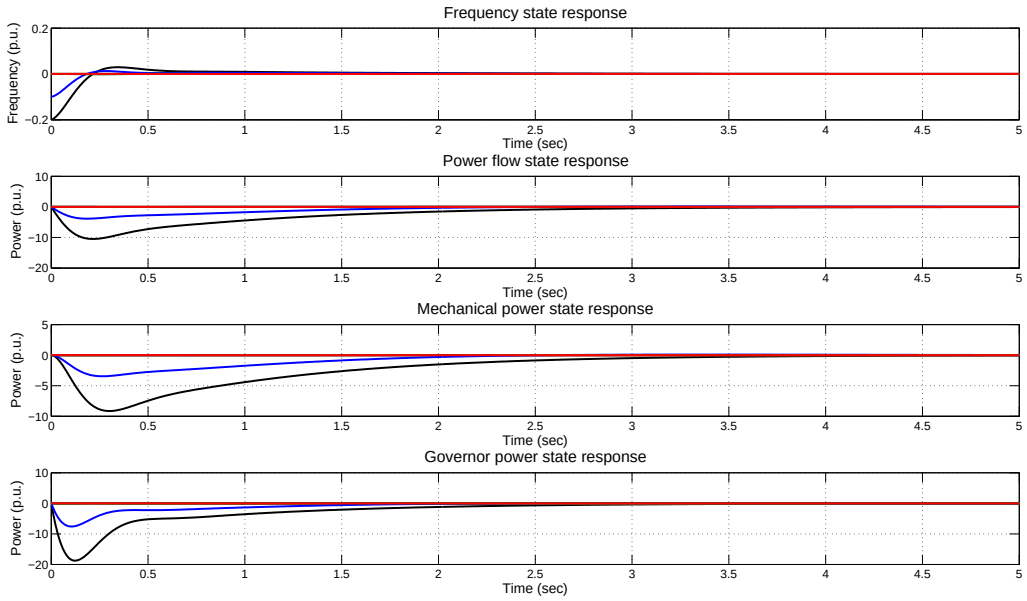

Figure 33: Control (optimal structure) system response to a non-zero initial condition in Areas 4 and 8.

Table 6: The eigenvalues, natural frequencies, and damping ratios for the optimal structure

Eigenvalue	**Frequency (Hz)**	**Damping ratio**
-0.72108	0.11476	1.00
-0.74444	0.11848	1.00
-0.8088	0.12872	1.00
-1.0575	0.16831	1.00
-4.3211	0.68773	1.00
-7.5767	1.2059	1.00
-7.847	1.2489	1.00
-22.519	3.584	1
$-0.71833 \pm j0.39834$	0.13073	0.87453
$-1.3373 \pm j0.20232$	0.21526	0.98875
$-1.0763 \pm j0.93613$	0.22703	0.75454
$-1.5512 \pm j0.29733$	0.25137	0.98212
$-1.8488 \pm j0.399$	0.30102	0.97749
$-1.9307 \pm j0.70375$	0.32706	0.93953
$-5.2834 \pm j5.3005$	1.1911	0.70597
$-4.5556 \pm j8.1267$	1.4828	0.48898
$-4.9626 \pm j8.9686$	1.6313	0.48415
$-7.0743 \pm j7.4667$	1.6370	0.68777
$-7.0626 \pm j8.0457$	1.7039	0.6597
$-7.8056 \pm j8.0436$	1.7839	0.69641
$-7.1454 \pm j8.8194$	1.8065	0.62951
$-7.5779 \pm j8.7012$	1.8364	0.65675
$-8.3967 \pm j11.02$	2.2050	0.60608
$-8.9823 \pm j12.007$	2.3865	0.59903

Table 7: Control laws for the ten controllers.

Area	Note
$u_1(t) = K_1 X_1(t)$	$K_1 = [K_{11}, K_{13}, K_{14}, K_{15}, K_{17}, K_{18}, K_{19}, K_{110}]$ and $X_1(t) = \left[x_1(t); x_3^d(t); x_4^d(t); x_5^d(t); x_7^d(t); x_8^d(t); x_9^d(t); x_{10}^d(t)\right]$
$u_2(t) = K_2 X_2(t)$	$K_2 = [K_{21}, K_{22}, K_{23}, K_{24}]$ and $X_2(t) = \left[x_1^d(t); x_2(t); x_3^d(t), x_4^d(t)\right]$
$u_3(t) = K_3 X_3(t)$	$K_3 = [K_{33}]$ and $X_3 = [x_3(t)]$
$u_4(t) = K_4 X_4(t)$	$K_4 = [K_{41}, K_{43}, K_{44}]$ and $X_4(t) = \left[x_1^d(t); x_3^d(t); x_4(t)\right]$
$u_5(t) = K_5 X_5(t)$	$K_5 = [K_{55}]$ and $X_5(t) = [x_5(t)]$
$u_6(t) = K_6 X_6(t)$	$K_6 = [K_{66}]$ and $X_6(t) = [x_6(t)]$
$u_7(t) = K_7 X_7(t)$	$K_7 = [K_{72}, K_{73}, K_{74}, K_{77}, K_{710}]$ and $X_7(t) = \left[x_2^d(t); x_3^d(t); x_4^d(t); x_7(t); x_{10}^d(t)\right]$
$u_8(t) = K_8 X_8(t)$	$K_8 = [K_{83}, K_{88}]$ and $X_8(t) = \left[x_3^d(t); x_8(t)\right]$
$u_9(t) = K_9 X_9(t)$	$K_9 = [K_{94}, K_{99}, K_{910}]$ and $X_9(t) = \left[x_4^d(t); x_9(t); x_{10}^d(t)\right]$
$u_{10}(t) = K_{10} X_{10}(t)$	$K_{10} = [K_{102}, K_{103}, K_{104}, K_{1010}]$ and $X_{10}(t) = \left[x_2^d(t); x_3^d(t); x_4^d(t); x_{10}(t)\right]$
where K_{ii} and x_i are the gain matrix and state vector for local controller i, respectively. K_{ij} is the gain matrix assigned to the state information (x_j^d) which is sent from node j.	

6.2 DISCUSSION

The main purpose of this section is to compare the performance of our optimal structure with those of random fixed structures, a completely decentralized structure, and a centralized structure. For the purpose of this comparison, the fixed structures were randomly chosen, as shown in Figure 34, with the exception the "Y" structure, for which we allowed the same areas to be connected through tie-lines, enabling additional communication, as shown previously in Figure 18. Each small square represents a subsystem (area). For example in the "Y" structure, Subsystem 1 sends local state variables to Subsystems 2,3, and 4, and receives their state variables. We applied the same paradigm to all other subsystems. Figure 35 shows the dimensions of each single controller in the control structure.

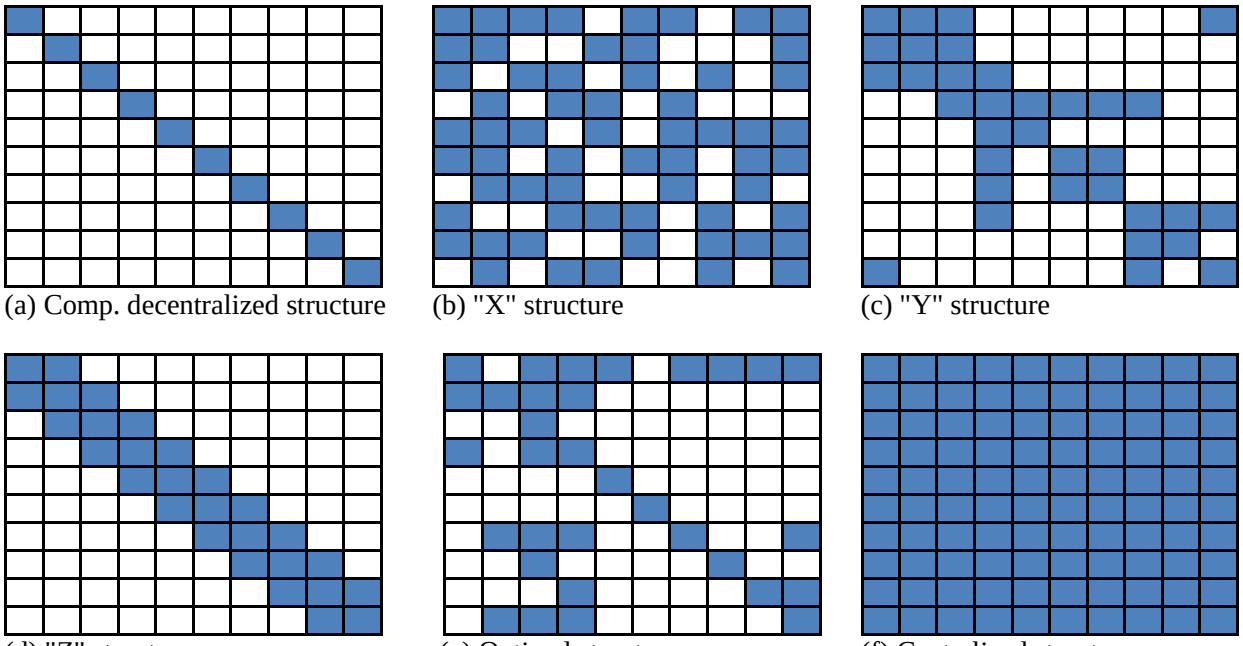

Figure 34: Various control structures.

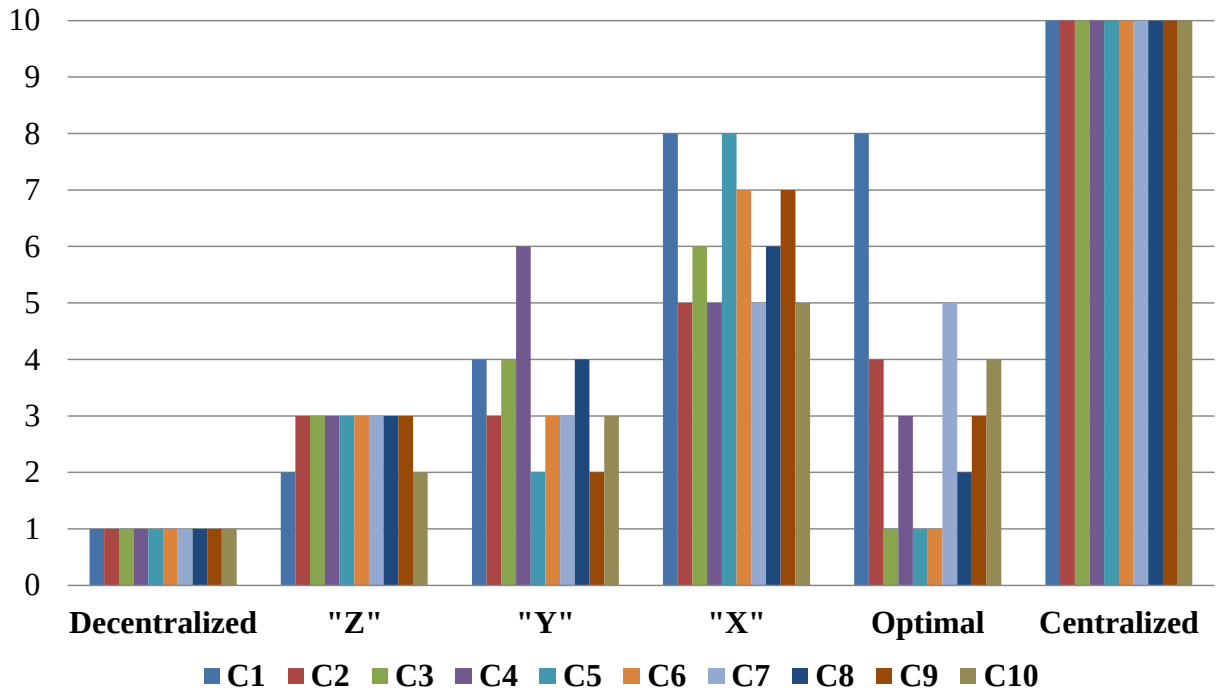

Figure 35: Controllers dimensions for all control structures.

Figures 38, 39, 40, 41, and 42 illustrate that the feedback control designed for all structures were able to stabilize the system by returning the disturbance states to zero steady state when non-zero initial frequency conditions were created in Areas 4 and 8. However, there are significant differences between these control structures. Figure 36 clearly supports the conclusion that the central controller represents significant additional damping of the system. Figure 29 shows a comparison between the control dimension and energy cost. The centralized structure has the lowest energy cost, but it has a full dimensional controller. On the other hand, the completely decentralized structure has the lowest controller dimension but entails high energy cost. When we moved from a completely decentralized structure to the "Z" structure by allowing some controllers to communicate, the energy cost is still high. By allowing more controllers to communicate as in the "Y" structure, we still were not

successful at decreasing the energy cost. This finding would indicate that adding unnecessary communication between controllers does not improve performance. Moving to the "X" structure by assigning more than half of the available communication channels improved the performance, but still did not guarantee getting the minimum energy cost. However, our model was able to obtain the best structure between controllers in order to meet power system stabilization requirements at minimum energy cost.

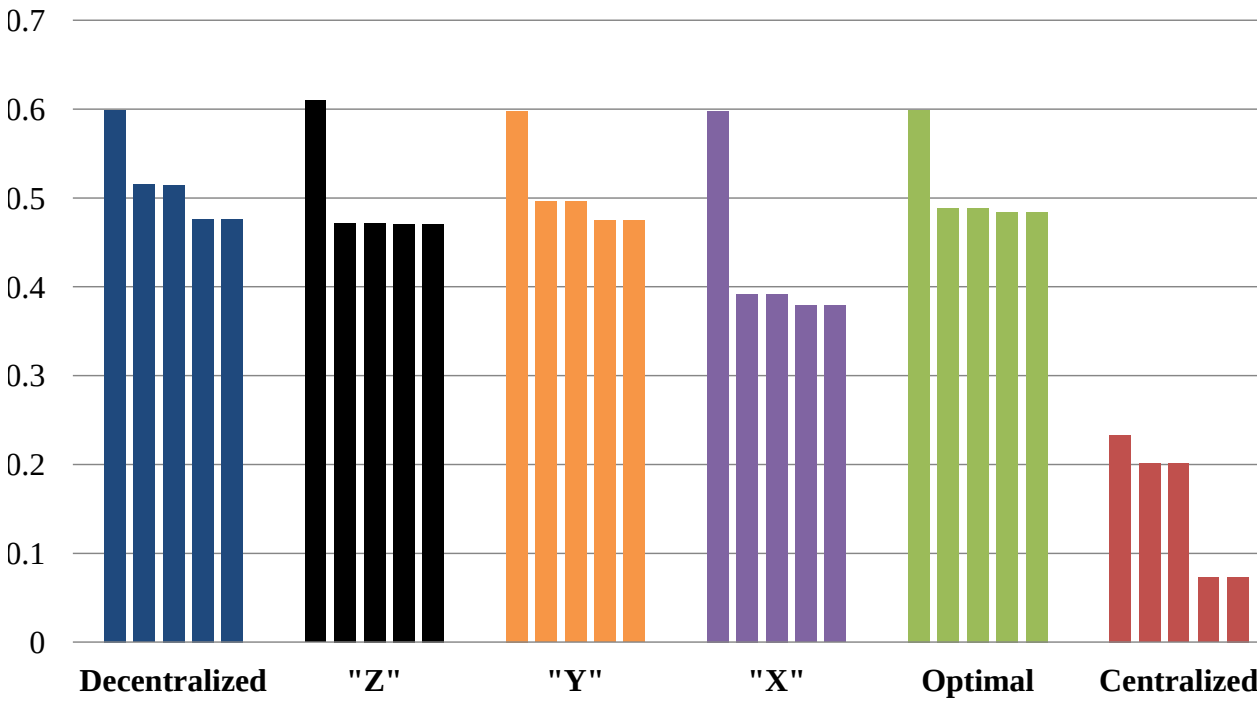

Figure 36: Lowest five damping ratios.

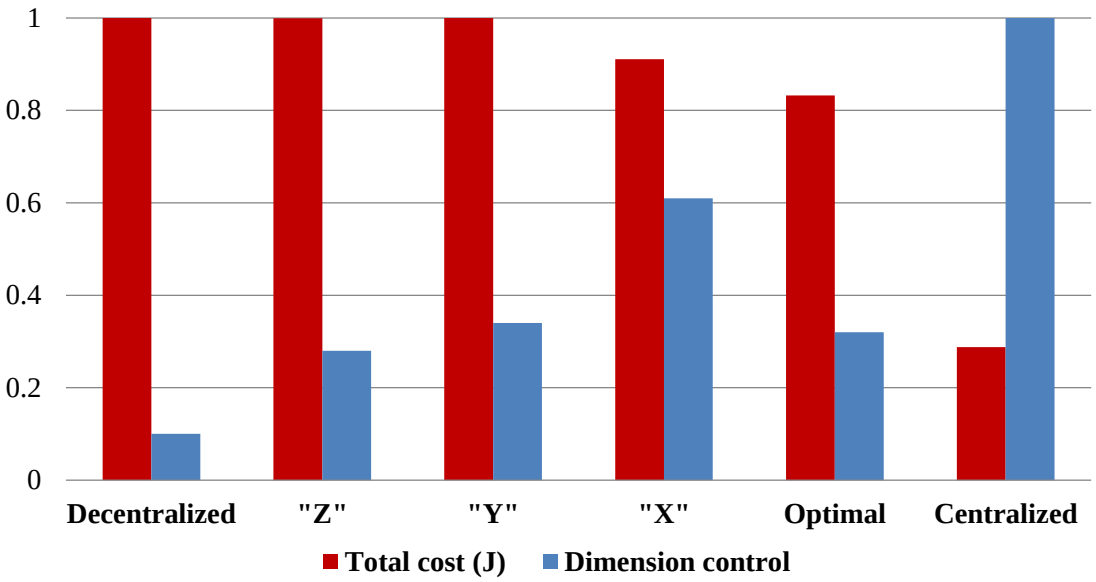

Figure 37: Total control dimension vs. energy cost for different control structures.

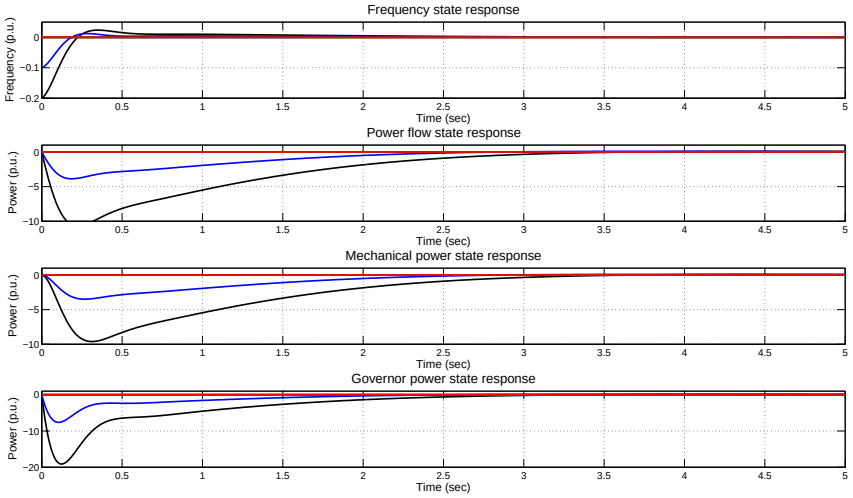

Figure 38: Control (completely decentralized structure) system response to a non-zero initial condition in Areas 4 and 8.

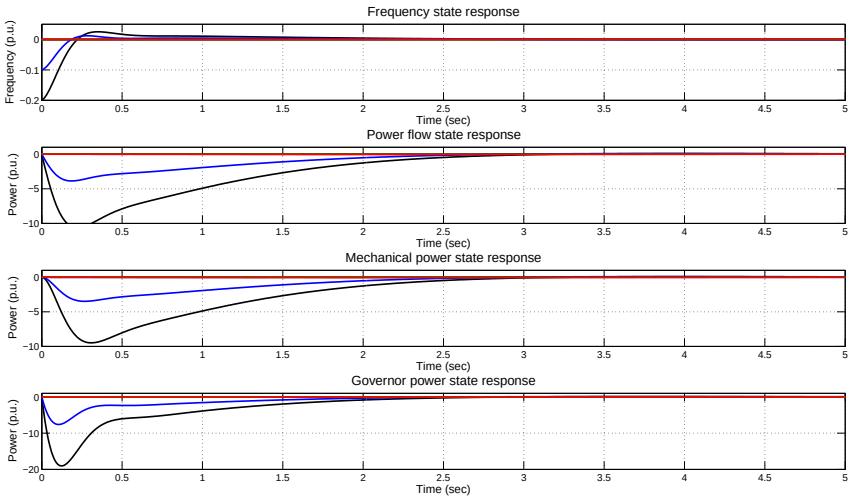

Figure 39: Control ("X" structure) system response to a non-zero initial condition in Areas 4 and 8.

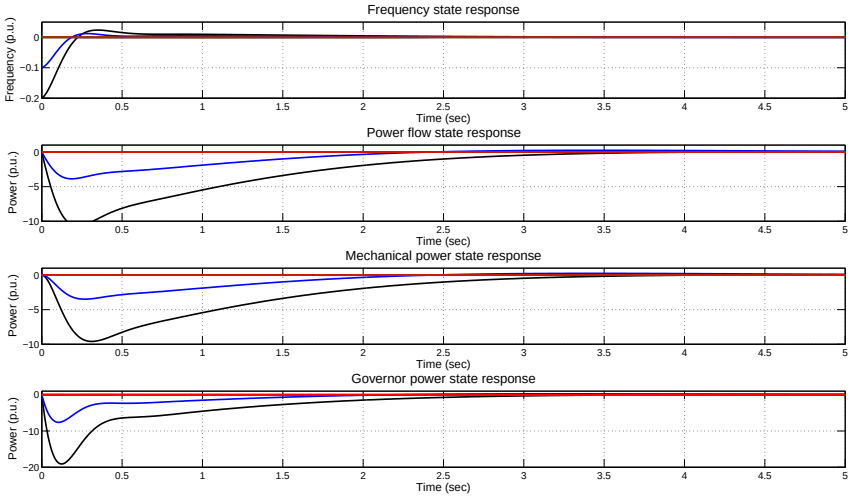

Figure 40: Control ("Y" structure) system response to a non-zero initial condition in Areas 4 and 8..

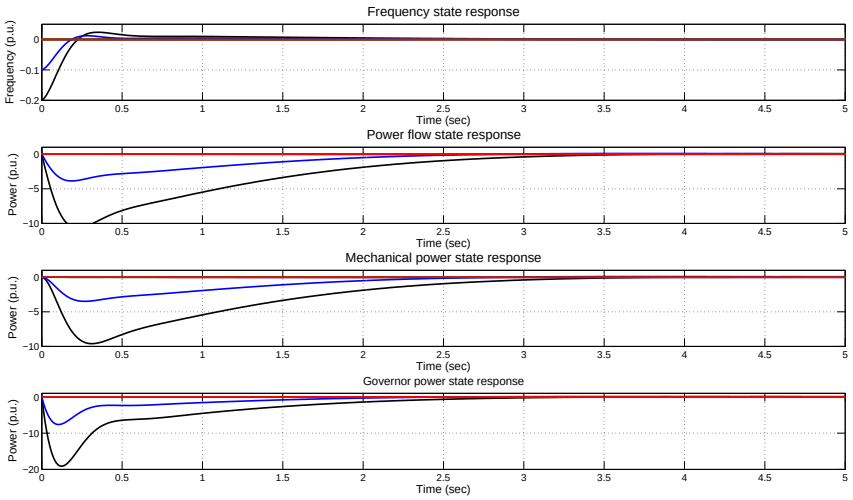

Figure 41: Control ("Z" structure) system response to a non-zero initial condition in Areas 4 and 8.

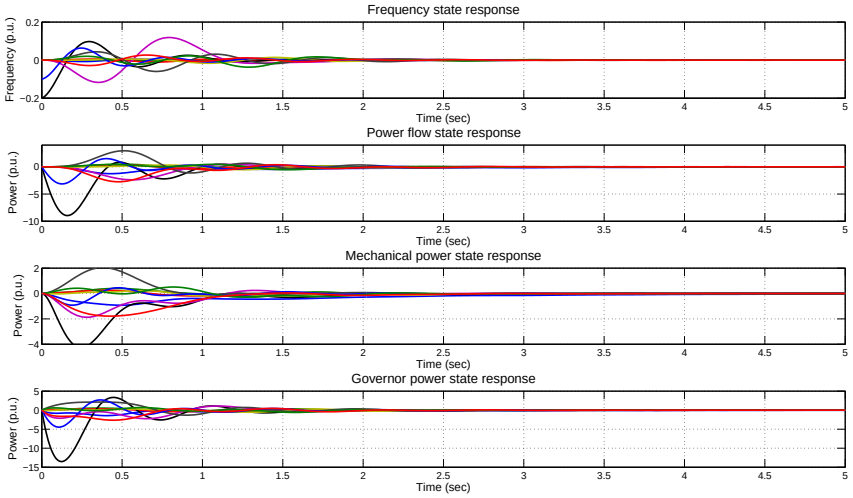

Figure 42: Control (centralized structure) system response to a non-zero initial condition in Areas 4 and 8.

7.0 CONCLUSION

Dimensionality reduction in a controller structure produces effective control signals with reduced computational load. In the control design of large-scale power systems, the manipulation of effective control signals, diminutive control dimensions, and suitable damping ratios presents a very challenging problem. The model we demonstrate in his thesis provides a solution to this challenge by integrating control and communication in the design of advance control structures for large-scale power systems. In particular, the control system present here avoids the potential ineffective performance of system based on fixed structures, which either include unnecessary communication channels or exclude essential communication channels between controllers. In our simulation, we have shown that the relationship between the control signal and the control dimension is based on system behavior. We were able to reduce the communication complexity of the control design and design a communication structure in order to achieve robust control.

Unlike other studies, in which the communication was indirectly reflected by a topology dependent matrix in the LQR cost function, our model considers the control structure and its communication channels in the cost function which helps to punish communication complexity of the controller structure. As a result our model was able to recognize communications as either essential or unessential during the design of the controller structure and thereby reduce the dimension of the controller. A design for distributed control, which is essential to suppressing inter-area low frequency oscillations in large-scale power systems, was presented in this thesis.

In the designing centralized or distributed control structures, communication constraints and time delay should be taken into account, in order to satisfy the performance specifications of a large-scale power system. Recent studies ignore the impact of time delay on the design

of robust control. If communication constraints and time delay are not considered in the design of such distributed control, system performance may be weak and may even cause instability in the system.

The design presented in this thesis creates innovative schemes for the system control design of a power system and is expected to contribute significantly to the national needs for power system control. First, this study integrates control and communication in the design of advanced control architectures for complex and large scale engineering systems, including the power system in this country and internationally. The principles, methods, and tools developed from this study enables the building of more complex systems and will ensure that these systems are reliable, efficient, and robust. Second, this study offers more applications in the field of power system control. The detailed implementation of the hierarchical control in this study can serve as a guideline, which can be readily generalized to other optimization and control problems in power systems, such as the optimal power flow problem [9] and the dynamic unit commitment problem [85]. Third, this study of control in complex networks will accelerate the progress of other research areas in complex networked systems, such as understanding network structure, understanding network dynamics, and predictive modeling and simulation for networks [20].

APPENDIX

MORE SIMULATION RESULTS

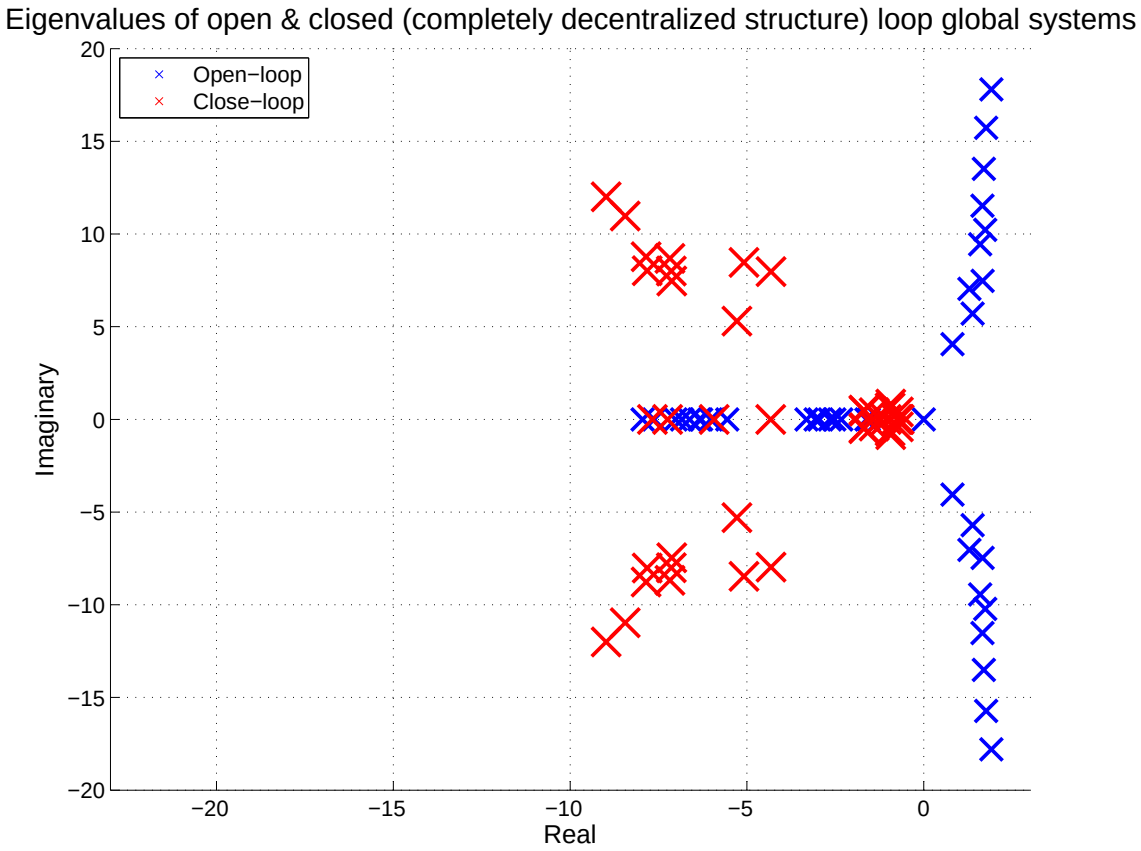

Figure 43: Eigenvalues of the closed-loop (decentralized structure) system.

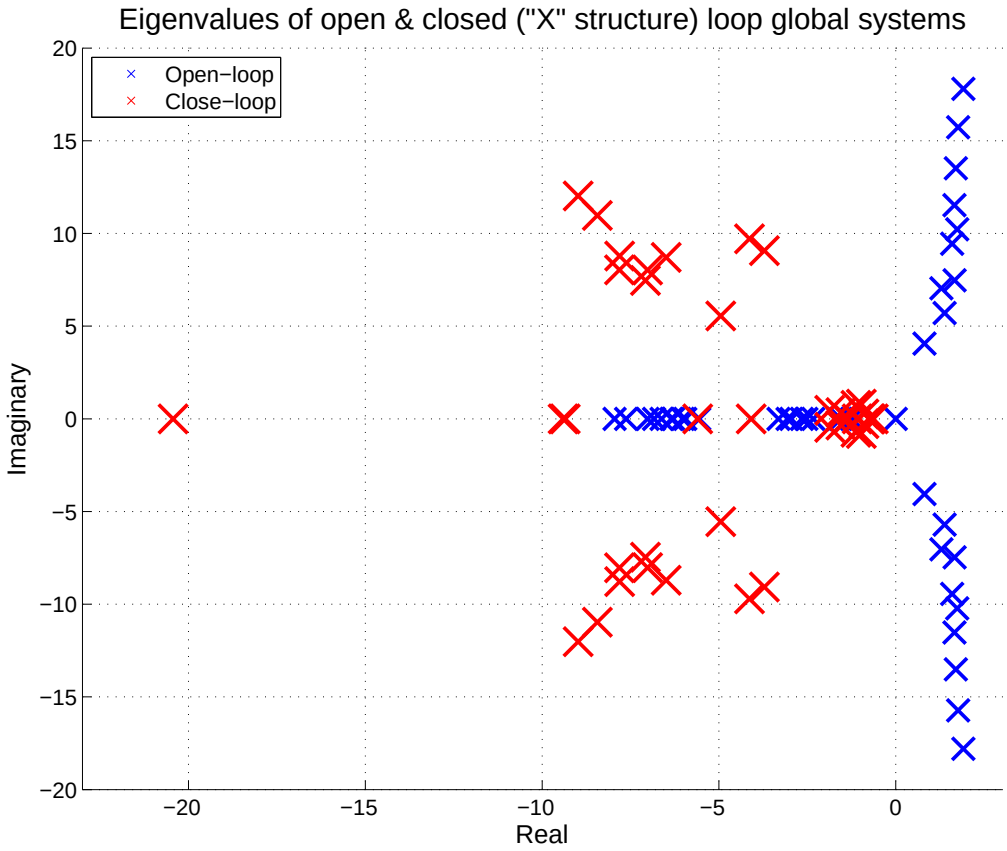

Figure 44: eigenvalues of the closed-loop (”X” structure) system.

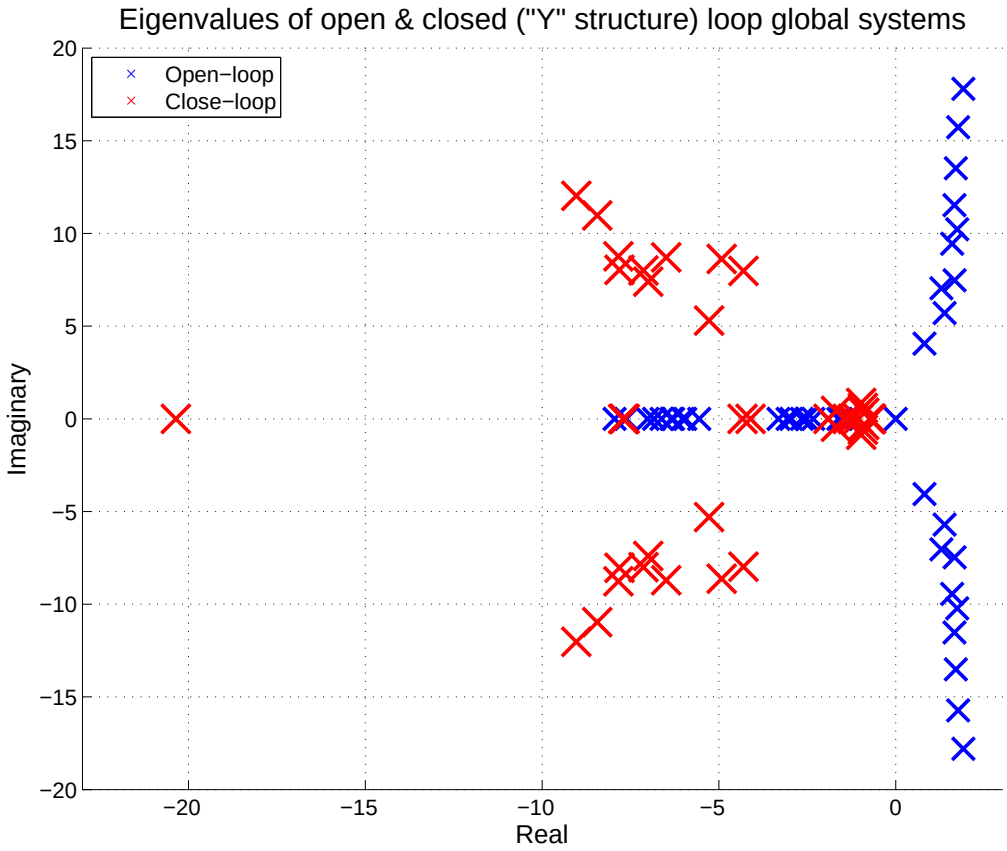

Figure 45: eigenvalues of the closed-loop ("Y" structure) system.

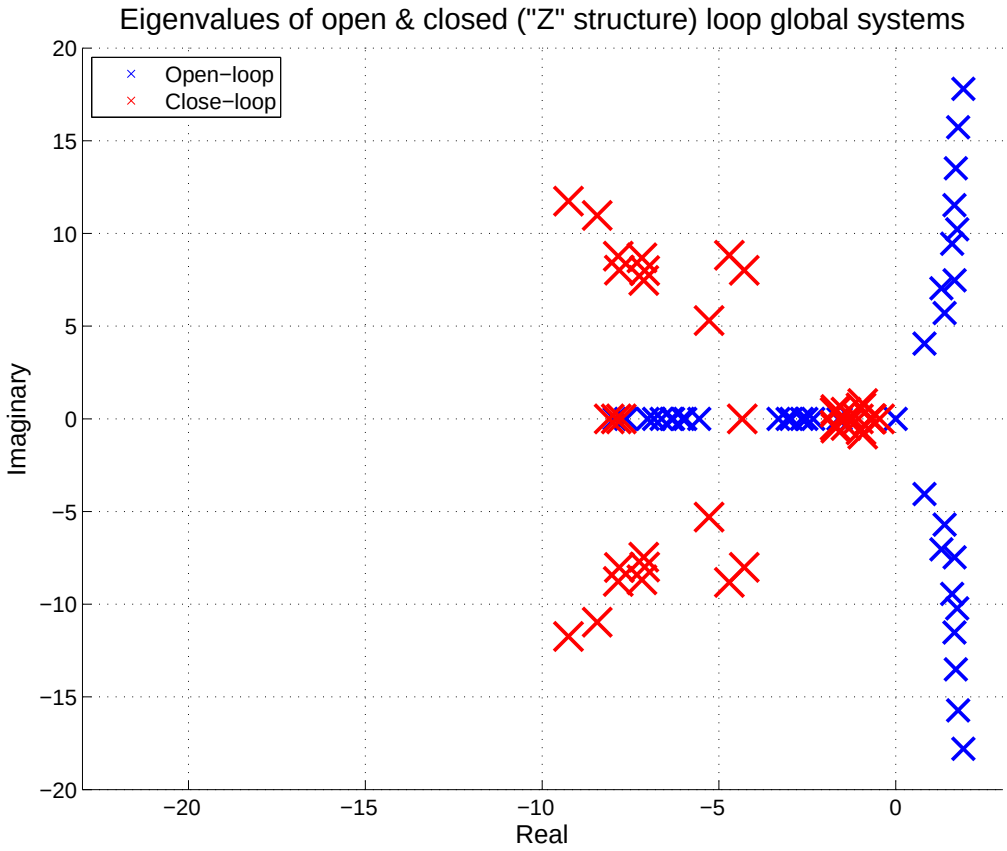

Figure 46: Eigenvalues of the closed-loop ("Z" structure) system.

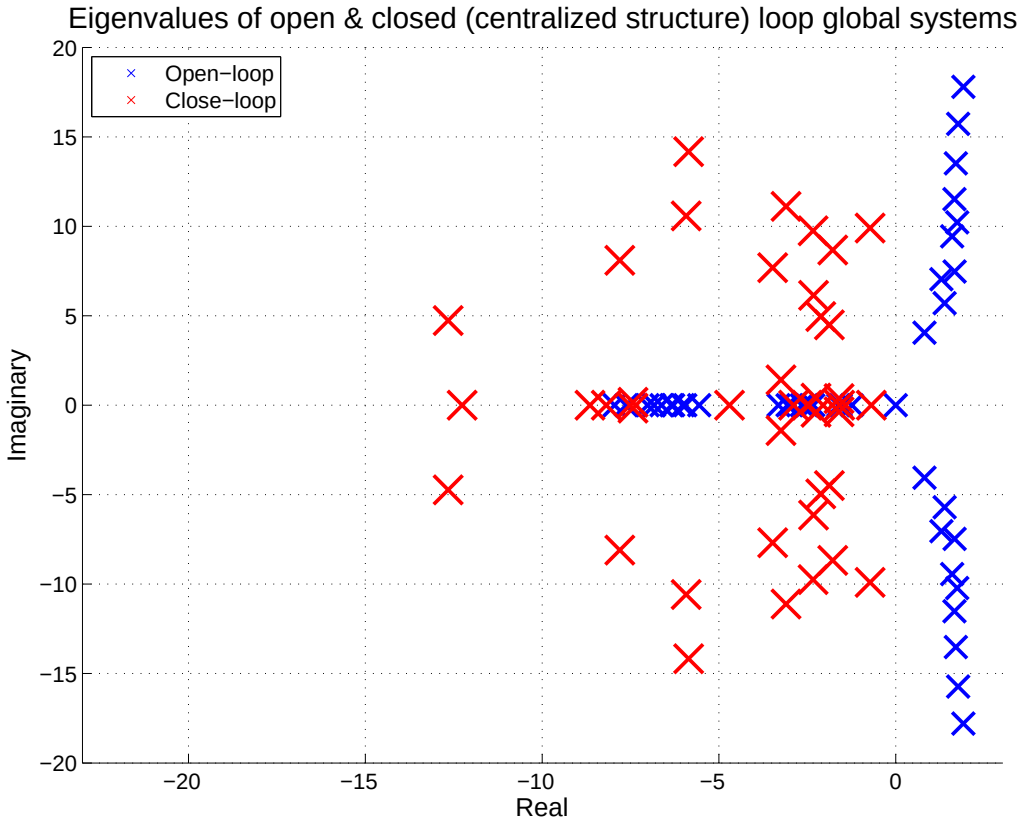

Figure 47: Eigenvalues of the closed-loop (centralized structure) system.

Table 8: The eigenvalues, natural frequencies, and damping ratios for the centralized structure.

Eigenvalue	**Frequency (Hz)**	**Damping ratio**
-0.69316	0.11032	1
-1.5874	0.25265	1
-2.5062	0.39887	1
-2.8874	0.45955	1
$-\ 4.7005$	0.74811	1
-8.1858	1.3028	1
-8.647	1.3762	1
$-\ 12.264$	1.9518	1
$-3.2465 \pm j1.4159$	0.5637	0.9166
$-1.6037 \pm j0.36607$	0.2618	0.9749
$-2.2552 \pm j0.3967$	0.36444	0.9848
$-1.8788 \pm j\ 4.4925$	0.77501	0.3858
$-2.1211 \pm j\ 4.9558$	0.85794	0.3934
$-2.324 \pm j6.1393$	1.0448	0.3540
$-7.428 \pm j0.16033$	1.1825	0.9997
$-3.4794 \pm j\ 7.6899$	1.3433	0.4122
$-1.7802 \pm j8.6778$	1.4099	0.2009
$-0.72728 \pm j\ 9.9041$	1.5805	0.0732
$-2.3382 \pm j\ 9.7529$	1.5962	0.2331
$-7.8041 \pm j\ 8.1038$	1.7906	0.6936
$-3.1033 \pm j\ 11.116$	1.8368	0.2689
$-5.9278 \pm j\ 10.585$	1.9308	0.4886
$-12.658 \pm j4.7356$	2.1510	0.9366
$-\ 5.8564 \pm j\ 14.168$	2.4400	0.3820

Table 9: The eigenvalues, natural frequencies, and damping ratios for the completely decentralized structure.

Eigenvalue	**Frequency (Hz)**	**Damping ratio**
-0.69428	0.1105	1
-0.72404	0.11523	1
-0.75599	0.12032	1
-1.0571	0.16824	1
-4.3295	0.68906	1
-5.9268	0.94327	1
-7.2437	1.1529	1
-7.6724	1.2211	1
$-0.71666 \pm j\ 0.40385$	0.13092	0.8712
$-0.95019 \pm j0.62198$	0.18075	0.8366
$-0.93525 \pm j0.82541$	0.19853	0.7497
$-1.4052 \pm j0.36455$	0.23104	0.9679
$-1.6828 \pm j0.45002$	0.27725	0.9660
$-1.6931 \pm j\ 0.50219$	0.28107	0.9587
$-5.283 \pm j5.3029$	1.1913	0.7057
$-4.3205 \pm j7.9709$	1.443	0.4765
$-5.082 \pm j8.4639$	1.5712	0.5147
$-7.1256 \pm j\ 7.4649$	1.6425	0.6904
$-7.139 \pm j8.0028$	1.7068	0.6656
$-7.8202 \pm j8.0183$	1.7826	0.6982
$-7.1796 \pm j8.6827$	1.7931	0.6372
$-7.8532 \pm j\ 8.771$	1.8737	0.6670
$-8.4416 \pm j\ 10.972$	2.2033	0.6097
$-8.9831 \pm j12.007$	2.3865	0.5990

Table 10: The eigenvalues, natural frequencies, and damping ratios for open-loop system.

Eigenvalue	**Frequency (Hz)**	**Damping ratio**
-1.2391	0.1972	1
-1.5548	0.2476	1
-2.3351	0.37163	1
-2.5308	0.40279	1
-2.656	0.42272	1
-2.9548	0.47027	1
-3.0597	0.48696	1
-3.3167	0.52787	1
-5.5592	0.88477	1
-5.9535	0.94753	1
-6.0219	0.95842	1
-6.2948	1.0019	1
-6.344	1.0097	1
-6.6197	1.0536	1
-6.8357	1.0879	1
-7.0185	1.117	1
-7.6245	1.2135	1
-7.9511	1.2655	1
3.6457e-16	5.8023e-17	-1
$0.81081 \pm j\ 4.0553$	0.65819	-0.19606
$1.383 \pm j\ 5.7033$	0.93401	-0.23566
$1.2899 \pm j\ 7.0433$	1.1396	-0.18015
$1.6634 \pm j\ 7.4759$	1.2189	-0.21719
$1.5923 \pm j\ 9.4434$	1.5242	-0.16627

Table 11: The eigenvalues, natural frequencies, and damping ratios for open-loop system (cont.).

Eigenvalue	**Frequency (Hz)**	**Damping ratio**
$1.7368 \pm j\ 10.225$	1.6507	-0.16746
$1.6581 \pm j\ 11.522$	1.8527	-0.14244
$1.6974 \pm j\ 13.516$	2.1681	-0.12461
$1.7646 \pm j\ 15.728$	2.5189	-0.1115
$1.9111 \pm j\ 17.801$	2.8494	-0.10674

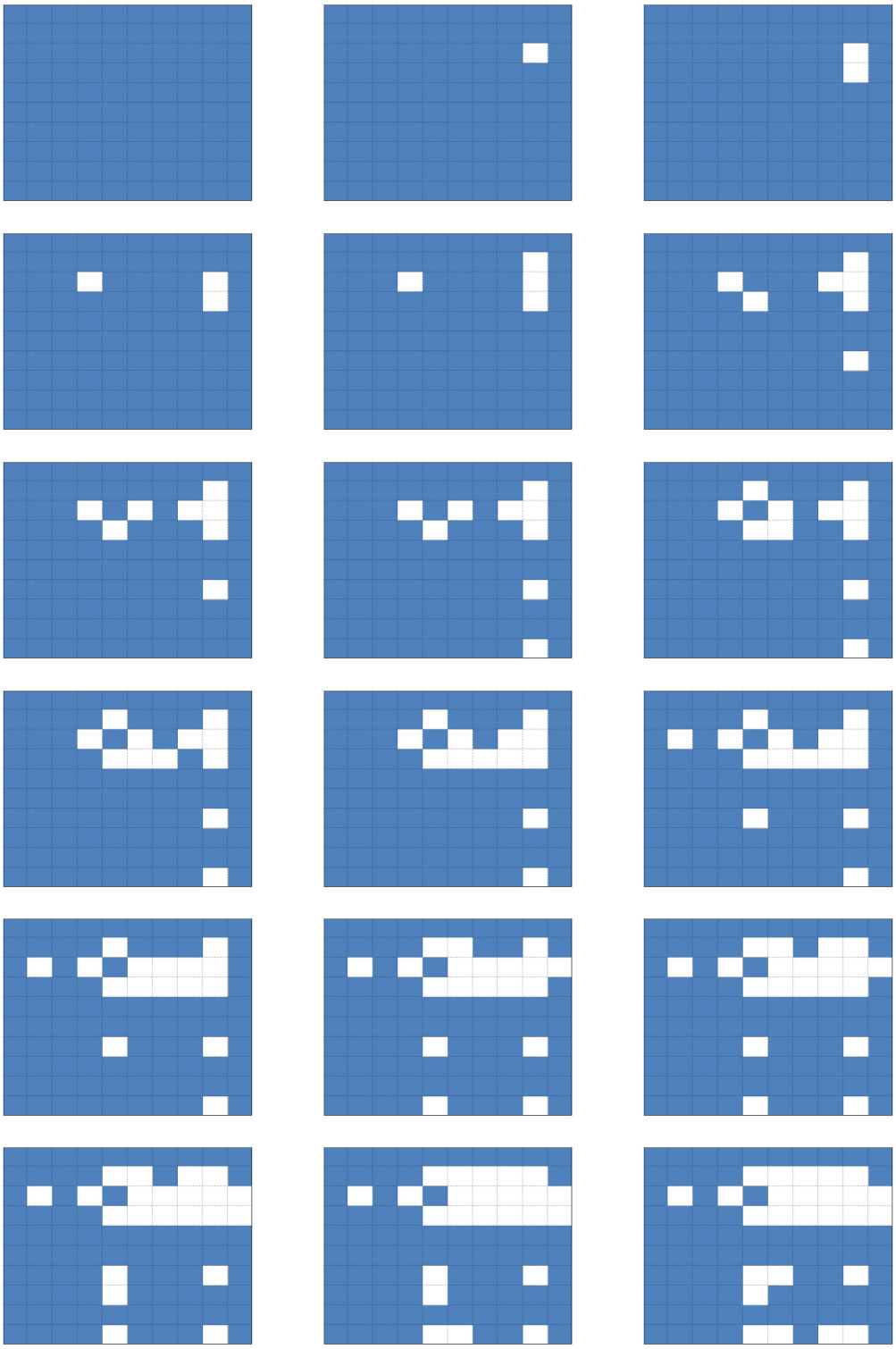

Figure 48: Feedback gain matrix structures during optimization development (part 1/3).

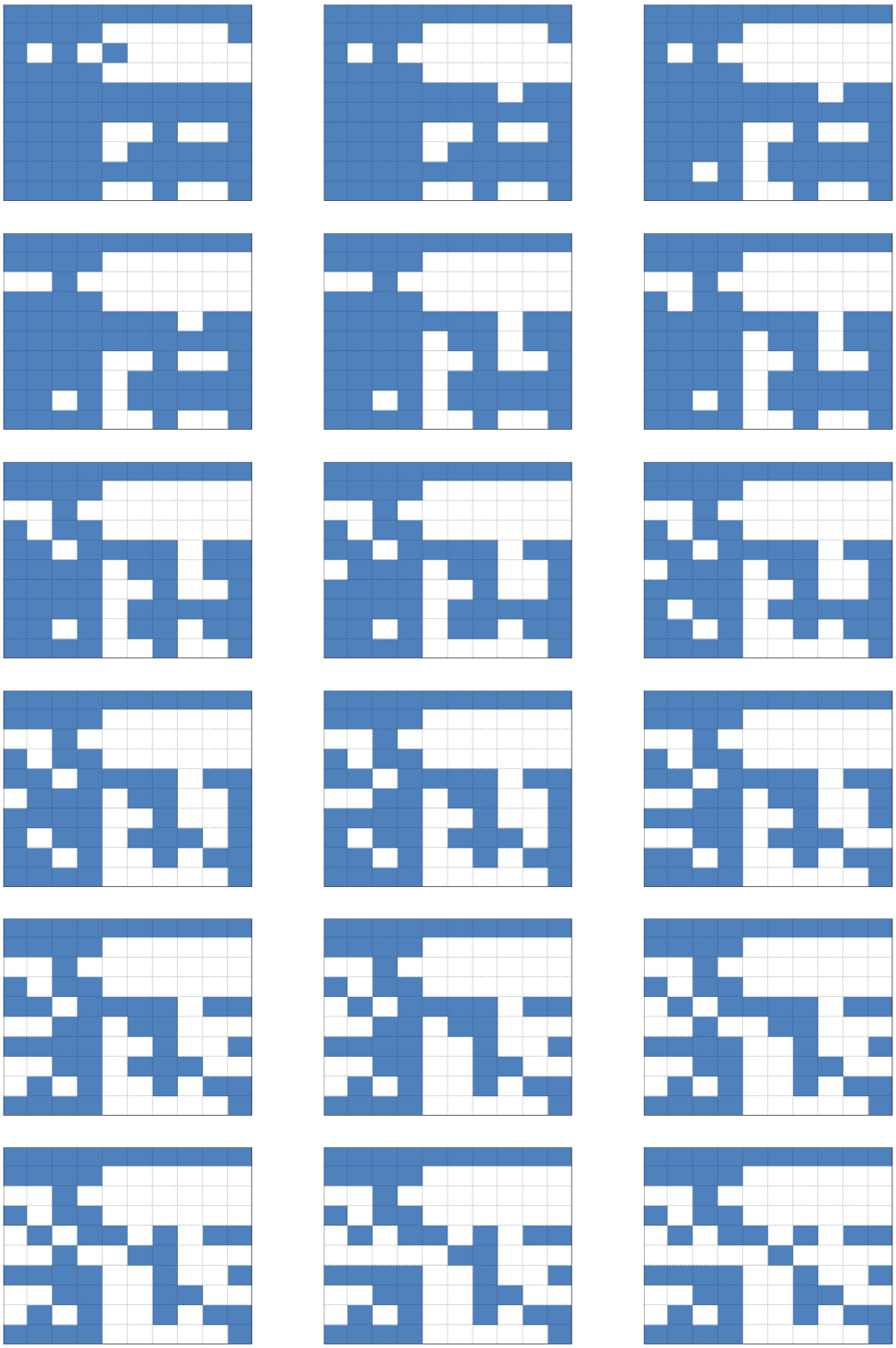

Figure 49: Feedback gain matrix structures during optimization development (part 2/3).

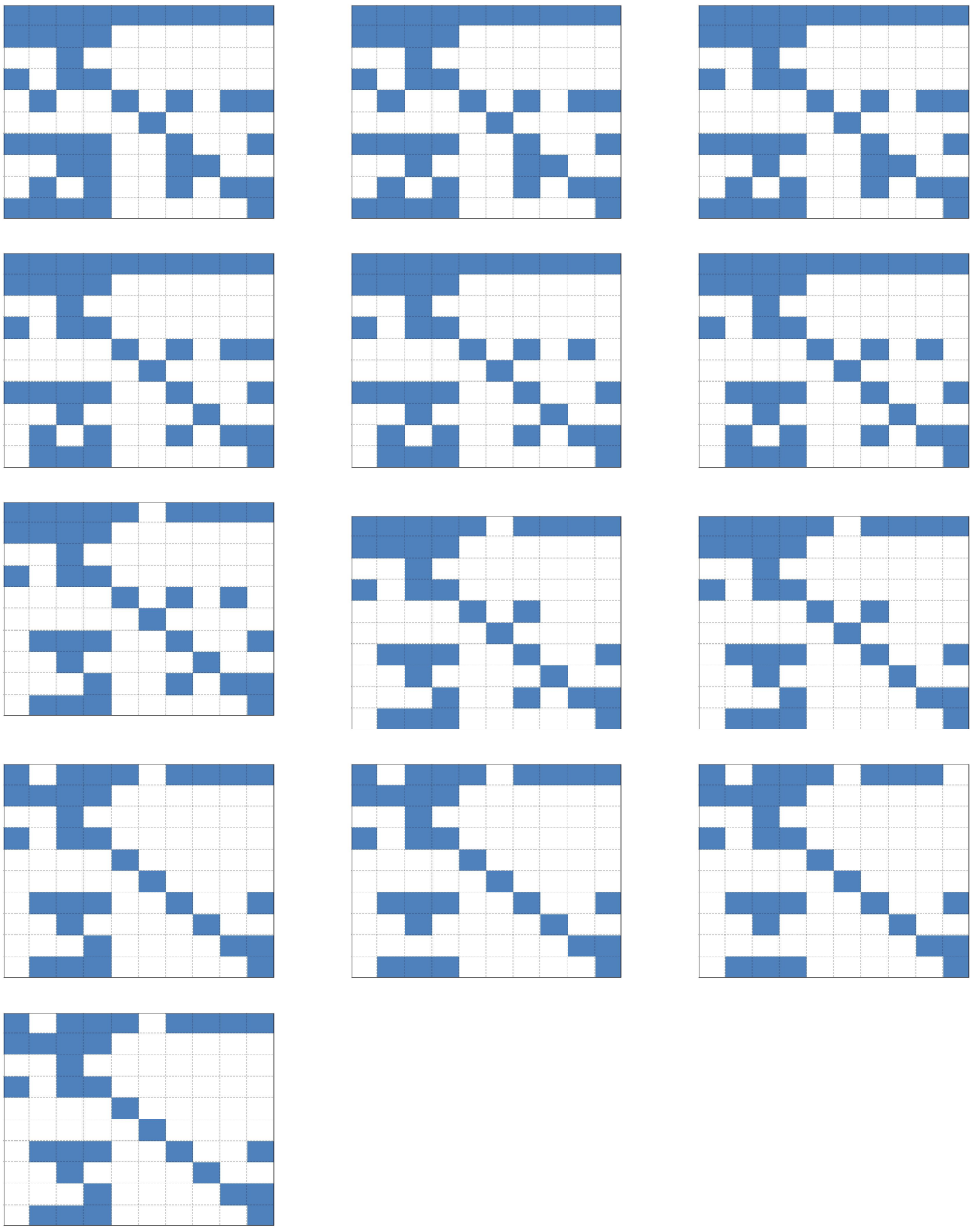

Figure 50: Feedback gain matrix structures during optimization development (part 3/3).

BIBLIOGRAPHY

[1] *The Earth Observatory is part of the EOS Project Science Office located at NASA Goddard Space Flight Center.*

[2] *U.S. National Grid Map.* Global Energy Network Institute.

[3] U S Energy Information Administration. *Annual Energy Outlook 2012, with Projections To 2035.* U.S. Government Printing Office, 2012.

[4] U S Energy Information Administration. *Early Release Overview of Annual Energy Outlook 2013, with Projections To 2040.* U.S. Government Printing Office, 2013.

[5] L.A. Aguirre. Quantitative measure of modal dominance for continuous systems. In *Decision and Control, 1993., Proceedings of the 32nd IEEE Conference on*, pages 2405 –2410 vol.3, dec 1993.

[6] B.D.O. Anderson and A.C. Antoulas. Rational interpolation and state variable realizations. In *Decision and Control, 1990., Proceedings of the 29th IEEE Conference on*, pages 1865 –1870 vol.3, dec 1990.

[7] A. C. Antoulas, D. C. Sorensen, and S. Gugercin. A survey of model reduction methods for large-scale systems. *Contemporary Mathematics*, 280:193–219, 2001.

[8] P. Antsaklis and J. Baillieul. Special issue on technology of networked control systems. *Proceedings of the IEEE*, 95(1):5 –8, jan. 2007.

[9] A.M. Azmy. Optimal power flow to manage voltage profiles in interconnected networks using expert systems. *Power Systems, IEEE Transactions on*, 22(4):1622 –1628, nov. 2007.

[10] W. Bajwa, J. Haupt, A. Sayeed, and R. Nowak. Joint source-channel communication for distributed estimation in sensor networks. *Information Theory, IEEE Transactions on*, 53(10):3629 –3653, oct. 2007.

[11] G.A. Baker. *Essentials of Padé approximants.* Academic Press, 1975.

[12] Mikhail Belkin and Partha Niyogi. Laplacian eigenmaps and spectral techniques for embedding and clustering. In *Advances in Neural Information Processing Systems 14*, pages 585–591. MIT Press, 2001.

[13] Wang Bo, Quanyuan Jiang, and Yijia Cao. Transmission network fault location using sparse pmu measurements. In *Sustainable Power Generation and Supply, 2009. SUPERGEN '09. International Conference on*, pages 1 –6, april 2009.

[14] K. Bollinger and R. Lalonde. Tuning synchronous generator voltage regulators using online generator models. *Power Apparatus and Systems, IEEE Transactions on*, 96(1):32–37, Jan.

[15] K.E. Bollinger, R. Winsor, and A. Campbell. Frequency response methods for tuning stabilizers to damp out tie-line power oscillations: Theory and field-test results. *Power Apparatus and Systems, IEEE Transactions on*, PAS-98(5):1509–1515, Sept.

[16] D. BONVIN and D. A. MELLICHAMP. A unified derivation and critical review of modal approaches to model reduction. *International Journal of Control*, 35(5):829–848, 1982.

[17] S. Boyd, L. El Ghaoui, E. Feron, and V. Balakrishnan. *Linear Matrix Inequalities in System and Control Theory*, volume 15 of *Studies in Applied Mathematics*. SIAM, Philadelphia, PA, June 1994.

[18] S. Boyd, L.E. Ghaoul, E. Feron, and V. Balakrishnan. *Linear Matrix Inequalities in System and Control Theory*. Siam Studies in Applied Mathematics. Society for Industrial and Applied Mathematics, 1994.

[19] Matthew Brand. Charting a manifold. In *Advances in Neural Information Processing Systems 15*, pages 961–968. MIT Press, 2003.

[20] James M. Brase and David L. Brown. Modeling, simulation and analysis ofcomplex networked systems: A program plan. 2009.

[21] Dennis J. Brueni and Lenwood S. Heath. The pmu placement problem. *SIAM J. Discret. Math.*, 19(3):744–761, July 2005.

[22] E.J. Candes, J. Romberg, and T. Tao. Robust uncertainty principles: exact signal reconstruction from highly incomplete frequency information. *Information Theory, IEEE Transactions on*, 52(2):489 – 509, feb. 2006.

[23] E.J. Candes and M.B. Wakin. An introduction to compressive sampling. *Signal Processing Magazine, IEEE*, 25(2):21 –30, march 2008.

[24] D. Chaniotis and M.A. Pai. Model reduction in power systems using krylov subspace methods. *Power Systems, IEEE Transactions on*, 20(2):888 – 894, may 2005.

[25] N.R. Chaudhuri, B. Chaudhuri, S. Ray, and R. Majumder. Wide-area phasor power oscillation damping controller: A new approach to handling time-varying signal latency. *Generation, Transmission Distribution, IET*, 4(5):620–630, May.

[26] C.T. Chen. *Linear System Theory and Design.* The Oxford Series In Electrical And Computer Engineering. Oxford University Press, 1999.

[27] J.H. Chow, Juan J. Sanchez-Gasca, Haoxing Ren, and S. Wang. Power system damping controller design-using multiple input signals. *Control Systems, IEEE*, 20(4):82–90, Aug.

[28] T.F. Cox and M.A.A. Cox. *Multidimensional Scaling.* Monographs on Statistics and Applied Probability. Chapman & Hall/CRC, 2001.

[29] M. L. Crow, C. Gill, F. Liu, B. Mcmillin, D. Niehaus, and D. Tauritz. Engineering the advanced power grid: Research challenges and tasks. In *RTAS 2006 Workshop on Research Directions for Security and Networking in Critical Real-Time and Embedded Systems*, 2006.

[30] Vasudev Gharpure Damir Novosel Daniel Karlsson Mehmet Kaba David G. Hart, David Uy. Pmus a new approach to power network monitoring. *ABB Review*, pages 58–61, 2001.

[31] F.P. DeMello and Charles Concordia. Concepts of synchronous machine stability as affected by excitation control. *Power Apparatus and Systems, IEEE Transactions on*, PAS-88(4):316–329, April.

[32] David L. Donoho and Michael Elad. Optimally sparse representation in general (non-orthogonal) dictionaries via 1 minimization. In *Proc. Natl Acad. Sci. USA 100 2197202*, 2003.

[33] D.L. Donoho. Compressed sensing. *Information Theory, IEEE Transactions on*, 52(4):1289 –1306, april 2006.

[34] D. Dotta, A.S. e Silva, and I.C. Decker. Wide-area measurements-based two-level control design considering signal transmission delay. *Power Systems, IEEE Transactions on*, 24(1):208 –216, feb. 2009.

[35] H.G. Far, H. Banakar, Pei Li, Changling Luo, and Boon-Teck Ooi. Damping interarea oscillations by multiple modal selectivity method. *Power Systems, IEEE Transactions on*, 24(2):766–775, May.

[36] P. Gahinet, A. Nemirovski, A. J. Laub, and M. Chilali. LMI Control Toolbox: For use with MATLAB. 1995.

[37] A.J. Germond and R. Podmore. Dynamic aggregation of generating unit models. *Power Apparatus and Systems, IEEE Transactions on*, PAS-97(4):1060–1069, July.

[38] J.C. Geromel, J. Bernussou, and P.L.D. Peres. Decentralized control through parameter space optimization. *Automatica*, 30(10):1565 – 1578, 1994.

[39] G.H. Golub and C.F. Van Loan. *Matrix Computations*. Johns Hopkins Studies in the Mathematical Sciences. Johns Hopkins University Press, 1996.

[40] B. Gou. Generalized integer linear programming formulation for optimal pmu placement. *Power Systems, IEEE Transactions on*, 23(3):1099 –1104, aug. 2008.

[41] J. Haupt, W.U. Bajwa, M. Rabbat, and R. Nowak. Compressed sensing for networked data. *Signal Processing Magazine, IEEE*, 25(2):92 –101, march 2008.

[42] S. Haykin and E. Moulines. Special issue on large-scale dynamic systems. *Proceedings of the IEEE*, 95(5):849 –852, may 2007.

[43] Bruce A. Hendrickson and Margaret H. Wright. Mathematical research challenges in optimization of complex systems. 2006.

[44] S. Hirano, T. Michigami, A. Kurita, D.B. Klapper, N.W. Miller, J.J. Sanchez-Gasca, and T.D. Younkins. Functional design for a system-wide multivariable damping controller [for power systems]. *Power Systems, IEEE Transactions on*, 5(4):1127–1136, Nov.

[45] D.D. iljak and A.I. Zeevi. Control of large-scale systems: Beyond decentralized feedback. *Annual Reviews in Control*, 29(2):169 – 179, 2005.

[46] The NETL Modern Grid Initiative. A systems view of the modern grid. 2007.

[47] A. Ishchenko, J.M.A. Myrzik, and W.L. Kling. Dynamic equivalencing of distribution networks with dispersed generation using hankel norm approximation. *Generation, Transmission Distribution, IET*, 1(5):818 –825, september 2007.

[48] M. Jamshidi. *Large-scale systems: modeling, control, and fuzzy logic*. Prentice Hall series on environmental and intelligent manufacturing systems. Prentice Hall, 1997.

[49] I.T. Jolliffe. *Principal Component Analysis*. Springer Series in Statistics. Springer-Verlag, 2002.

[50] I. Kamwa, R. Grondin, D. Asber, J.P. Gingras, and G. Trudel. Active-power stabilizers for multimachine power systems: challenges and prospects. *Power Systems, IEEE Transactions on*, 13(4):1352–1358, Nov.

[51] I. Kamwa, R. Grondin, and Y. Hebert. Wide-area measurement based stabilizing control of large power systems-a decentralized/hierarchical approach. *Power Systems, IEEE Transactions on*, 16(1):136–153, Feb.

[52] P.C. Krause and J.N. Towle. Synchronous machine damping by excitation control with direct and quadrature axis field windings. *Power Apparatus and Systems, IEEE Transactions on*, PAS-88(8):1266–1274, Aug.

[53] P. Kundur, N.J. Balu, and M.G. Lauby. *Power system stability and control*. The EPRI power system engineering series. McGraw-Hill, 1994.

[54] P. Kundur, M. Klein, G.J. Rogers, and M.S. Zywno. Application of power system stabilizers for enhancement of overall system stability. *Power Systems, IEEE Transactions on*, 4(2):614–626, May.

[55] Cédric Langbort and Vijay Gupta. Minimal interconnection topology in distributed control design. *SIAM J. Control Optim.*, 48(1):397–413, February 2009.

[56] E.V. Larsen and D. A. Swann. Applying power system stabilizers part i: General concepts. *Power Apparatus and Systems, IEEE Transactions on*, PAS-100(6):3017–3024, June.

[57] E.V. Larsen and D. A. Swann. Applying power system stabilizers part ii: Performance objectives and tuning concepts. *Power Apparatus and Systems, IEEE Transactions on*, PAS-100(6):3025–3033, June.

[58] E.V. Larsen and D. A. Swann. Applying power system stabilizers part iii: Practical considerations. *Power Apparatus and Systems, IEEE Transactions on*, PAS-100(6):3034–3046, June.

[59] M.H.C. Law and A.K. Jain. Incremental nonlinear dimensionality reduction by manifold learning. *Pattern Analysis and Machine Intelligence, IEEE Transactions on*, 28(3):377 –391, march 2006.

[60] J. Lfberg. Yalmip : A toolbox for modeling and optimization in MATLAB. In *Proceedings of the CACSD Conference*, Taipei, Taiwan, 2004.

[61] Chao Lu, Jennie Si, Xiaochen Wu, and Peng Li. Approximate dynamic programming coordinated control in multi-infeed hvdc power system. In *Power Systems Conference and Exposition, 2006. PSCE '06. 2006 IEEE PES*, pages 2131 –2135, 29 2006-nov. 1 2006.

[62] J. Machowski, J. Bialek, and J.R. Bumby. *Power system dynamics and stability*. John Wiley, 1997.

[63] N. Martins, L.T.G. Lima, and H.J.C.P. Pinto. Computing dominant poles of power system transfer functions. *Power Systems, IEEE Transactions on*, 11(1):162 –170, feb 1996.

[64] S. Mohagheghi, G.K. Venayagamoorthy, and R.G. Harley. Optimal wide area controller and state predictor for a power system. *Power Systems, IEEE Transactions on*, 22(2):693–705, May.

[65] J.A. Momoh. Smart grid design for efficient and flexible power networks operation and control. In *Power Systems Conference and Exposition, 2009. PSCE '09. IEEE/PES*, pages 1 –8, march 2009.

[66] B. Moore. Principal component analysis in linear systems: Controllability, observability, and model reduction. *Automatic Control, IEEE Transactions on*, 26(1):17 – 32, feb 1981.

[67] Y. Nesterov and A. Nemirovskii. *Interior Point Polynomial Algorithms in Convex Programming*. Studies in Applied and Numerical Mathematics. Society for Industrial and Applied Mathematics, 1987.

[68] Hui Ni, G.T. Heydt, and L. Mili. Power system stability agents using robust wide area control. *Power Systems, IEEE Transactions on*, 17(4):1123 – 1131, nov 2002.

[69] F. Okou, L-A Dessaint, and O. Akhrif. Power systems stability enhancement using a wide-area signals based hierarchical controller. *Power Systems, IEEE Transactions on*, 20(3):1465–1477, Aug.

[70] International Conference on Large High Voltage Electric Systems. *Analysis and Control of Power System Oscillations: Final Report*. CIGRE technical brochure. CIGRE, 1996.

[71] B. Pal and B. Chaudhuri. *Robust Control in Power Systems*. Power Electronics and Power Systems. Springer, 2005.

[72] B. Pal and B. Chaudhuri. *Robust Control in Power Systems*. Power Electronics And Power Systems. Springer, 2005.

[73] F. Palacios-Quinonero and J. M. Rossell. Decentralized control with information structure constraints. *15th International Workshop on Dynamics and Control*, 2009.

[74] Wei Qiao, Ganesh K. Venayagamoorthy, and Ronald G. Harley. Optimal wide-area monitoring and nonlinear adaptive coordinating neurocontrol of a power system with wind power integration and multiple facts devices. *Neural Networks*, 21(23):466 – 475, 2008.

[75] Chawasak Rakpenthai, Suttichai Premrudeepreechacharn, Sermsak Uatrongjit, and Neville R. Watson. An optimal pmu placement method against measurement loss and branch outage. *Power Delivery, IEEE Transactions on*, 22(1):101 –107, jan. 2007.

[76] Sara Robinson. *The Power Grid: Fertile Ground for Math Research*. SIAM News, 2003.

[77] G. Rogers. *Power system oscillations*. Kluwer international series in engineering and computer science: Power electronics & power systems. Kluwer Academic, 2000.

[78] G. Rogers. *Power system oscillations*. Kluwer international series in engineering and computer science: Power electronics & power systems. Kluwer Academic, 2000.

[79] G. Rogers. Demystifying power system oscillations. *Computer Applications in Power, IEEE*, 9(3):30–35, Jul.

[80] Sam T. Roweis and Lawrence K. Saul. Nonlinear dimensionality reduction by locally linear embedding. *Science*, 290(5500):2323–2326, 2000.

[81] Jr. Sandell, N. and M. Athans. Solution of some nonclassical lqg stochastic decision problems. *Automatic Control, IEEE Transactions on*, 19(2):108 – 116, apr 1974.

[82] Jr. Sandell, N., P. Varaiya, M. Athans, and M. Safonov. Survey of decentralized control methods for large scale systems. *Automatic Control, IEEE Transactions on*, 23(2):108 – 128, apr 1978.

[83] J. Shawe-Taylor and N. Cristianini. *Kernel Methods for Pattern Analysis*. Cambridge University Press, 2004.

[84] D.D. Siljak. *Large-Scale Dynamic Systems: Stability and Structure*. Dover Civil and Mechanical Engineering Series. Dover Publications, 2007.

[85] T.K. Siu, G.A. Nash, and Z.K. Shawwash. A practical hydro dynamic unit commitment and loading model. In *Power Industry Computer Applications, 2001. PICA 2001. Innovative Computing for Power - Electric Energy Meets the Market. 22nd IEEE Power Engineering Society International Conference on*, pages 26 –29, 2001.

[86] J. F. Sturm. Using sedumi 1.02, a MATLAB toolbox for optimization over symmetric cones. *Optimization Methods and Software*, 11–12:625–653, 1999.

[87] Joshua B. Tenenbaum, Vin de Silva, and John C. Langford. A global geometric framework for nonlinear dimensionality reduction. *Science*, 290(5500):2319–2323, 2000.

[88] Li Teng, Hongyu Li, Xuping Fu, Wenbin Chen, and I-Fan Shen. Dimension reduction of microarray data based on local tangent space alignment. In *Cognitive Informatics, 2005. (ICCI 2005). Fourth IEEE Conference on*, pages 154 – 159, aug. 2005.

[89] T. Van Cutsem and C. Vournas. *Voltage Stability of Electric Power Systems*. Kluwer International Series in Engineering and Computer Science. Kluwer Academic Publishers, 1998.

[90] R. Witzmann. Damping of interarea oscillations in large interconnected power systems. *IPST 2001*, pages 411–416, 2001.

[91] Hansheng Wu. Decentralized adaptive robust control for a class of large-scale systems including delayed state perturbations in the interconnections. *Automatic Control, IEEE Transactions on*, 47(10):1745 – 1751, oct 2002.

[92] Hongxia Wu, K.S. Tsakalis, and G.T. Heydt. Evaluation of time delay effects to wide-area power system stabilizer design. *Power Systems, IEEE Transactions on*, 19(4):1935–1941, Nov.

[93] A.I. Zečević and D.D. Siljak. *Control Of Complex Systems: Structural Constraints and Uncertainty*. Communications and Control Engineering. Springer, 2010.

[94] A.I. Zeevi and D.D. iljak. Control design with arbitrary information structure constraints. *Automatica*, 44(10):2642 – 2647, 2008.

[95] Yang Zhang and A. Bose. Design of wide-area damping controllers for interarea oscillations. *Power Systems, IEEE Transactions on*, 23(3):1136–1143, Aug.

[96] M. Zima, M. Larsson, P. Korba, C. Rehtanz, and G. Andersson. Design aspects for wide-area monitoring and control systems. *Proceedings of the IEEE*, 93(5):980–996, May.

[97] R.D. Zimmerman, C.E. Murillo-Sanchez, and R.J. Thomas. Matpower: Steady-state operations, planning, and analysis tools for power systems research and education. *Power Systems, IEEE Transactions on*, 26(1):12 –19, feb. 2011.